RESULTS OF DEBRIS FLOW INVESTIGATIONS ON THE RECENT TIME SCALE

Harry M. Blijenberg[1]

THE STUDY AREA

The study area is situated in the southern French Alps near the Italian border (Fig.1). The research is mainly carried out in the basin drained by the Bachelard river and its tributaries, upstream of the hamlet of Morjuan (Fig.2a and b). This area, east to west 17 km, north to south 5-9 km, is largely situated within the limits of the Mercantour National Parc which was founded in 1979. The valley is thinly inhabited; human influence is mainly limited to some sheep grazing and tourism in summer. Abandoned cottages and fields are evidence for more intensive agricultural activities in the past. Trees, mainly Larix decidua, are found up to the tree limit situated at 2300-2400m. Above the tree limit alpine pastures can be found up to the highest summits in the area, near 3000m. Most summits are situated between 2700 and 2900 m. The Bachelard river, rising near the Col de la Cayolle in the southeast of the study area, flows north to Bayasse, where the valley floor is situated at 1780m. Here the river turns west, and finally turns north again, flowing into the Ubaye river near the village of Barcelonnette at an altitude of 1120m.

Rocks in the area are of sedimentary origin. Rock types include limestones, sandstones, flysch, conglomerates and marls. The oldest rocks are found near the valley floor. These are dark Jurassic marls, the so-called Terres Noires. On top of these highly erodible marls lie upper Jurassic limestones, followed by lower Cretaceous limestones and marls and then by upper Cretaceous to Eocene limestones and calcareous marls and schists. Finally a series of sandstones with conglomeratic banks, the Grès d'Annot dating from the Oligocene. These autochtonous rocks are overlain by flysch deposits from the upper Cretaceous belonging to a nappe called the Nappe de Parpaillon. At the base of this nappe fragments of other rocks are found. These fragments were dragged along by the nappe, coming from the east during the Eocene. Figure 3 presents the lithology of the study area.

During the Pleistocene an alternation of colder and warmer periods has taken place. In the cold periods the Bachelard Valley has been glaciated. Evidence of these glaciations are the typical U-shape of the upstream part of the valley and some morainic deposits on the lower slopes south-east of Bayasse. At the heads of the tributary valleys many cirques can be found. Nowadays, none of these cirques is occupied by a glacier. The downstream part of the valley is characterized by the deeply incised Bachelard river and its tributaries, forming deep and narrow gorges in the resistant flysch rocks. During the Holocene slope processes and fluvial/torrent

1 Department of Physical Geography, Utrecht University.

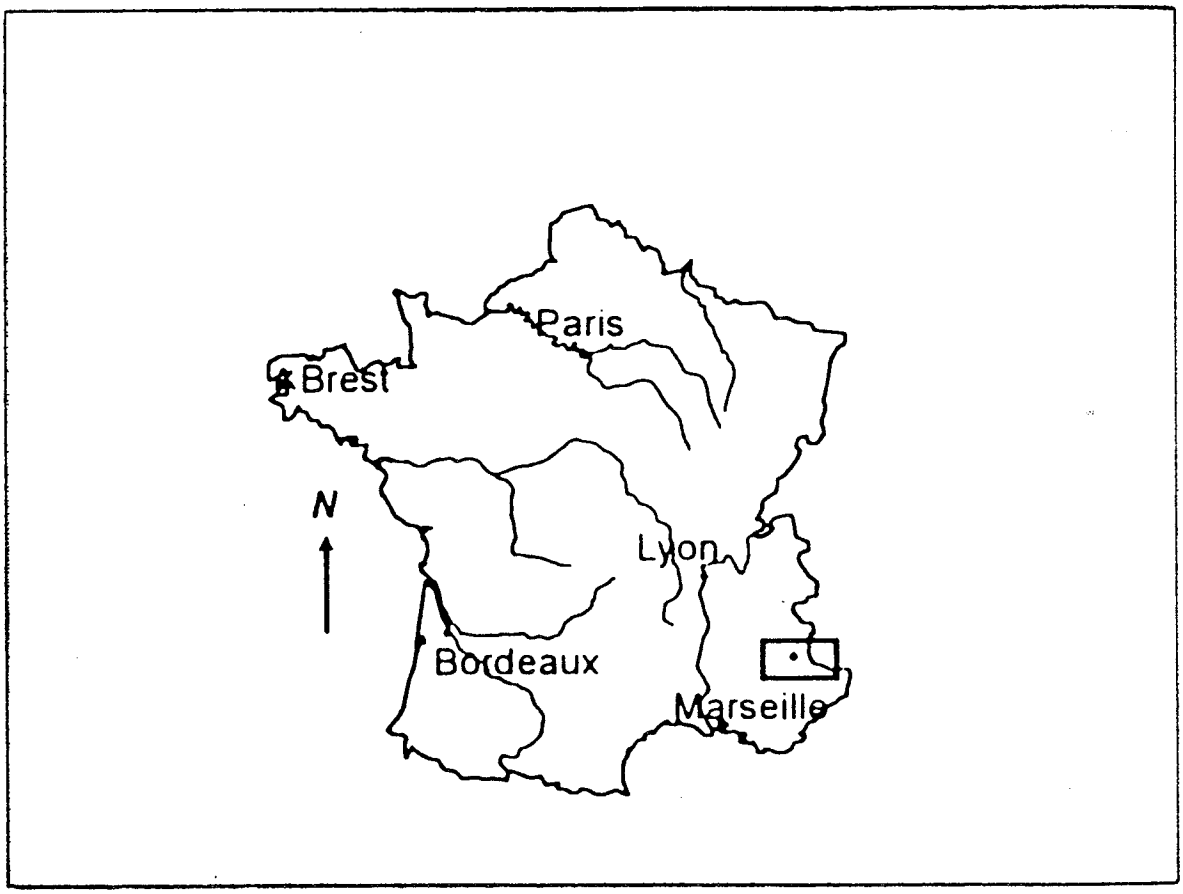

Figure 1: The location of the study area in France.

a: The Bachelard valley and its surroundings.

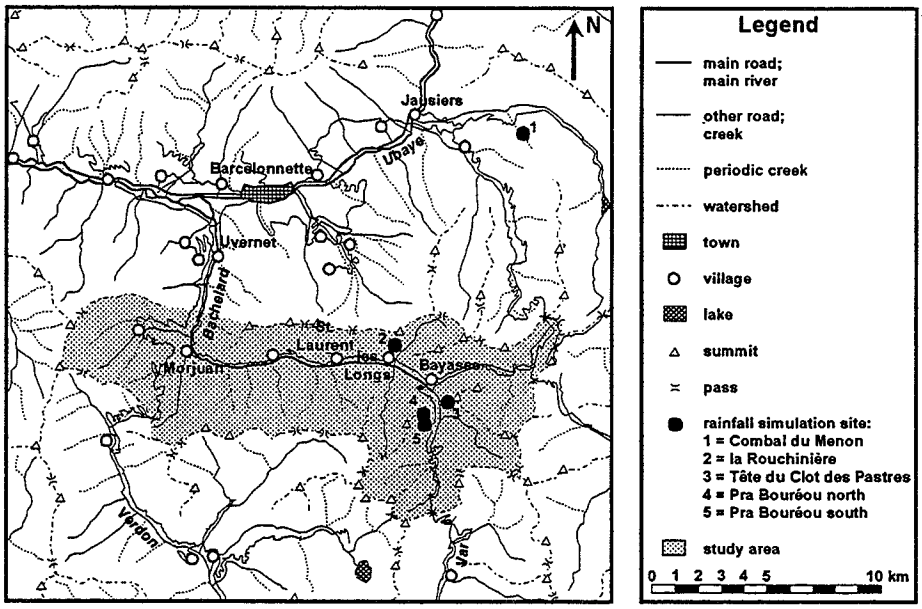

Figure 2: The study area.

b: The central part of the study area in the Bachelard valley.

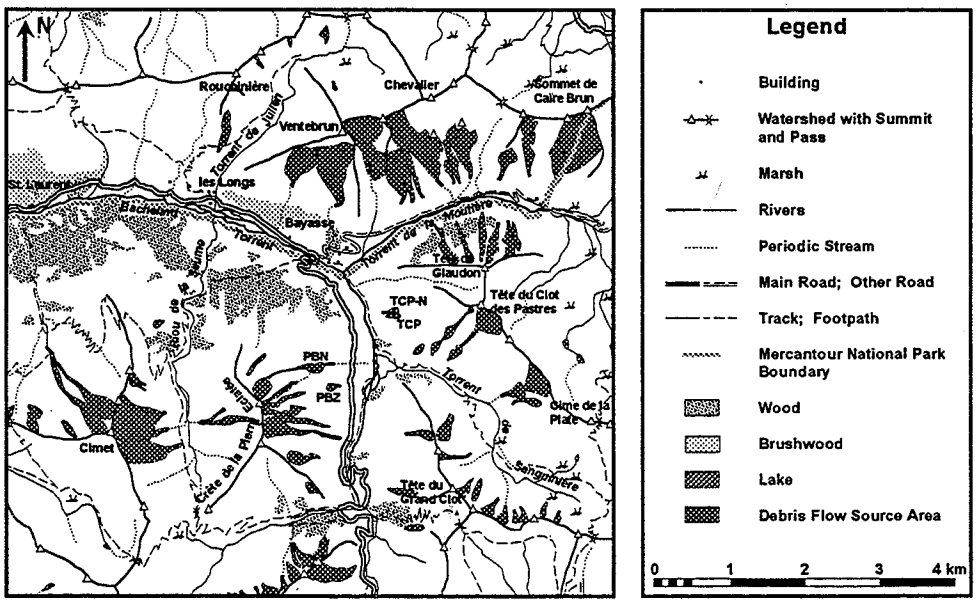

Figure 3: Lithological map of the Bachelard valley.

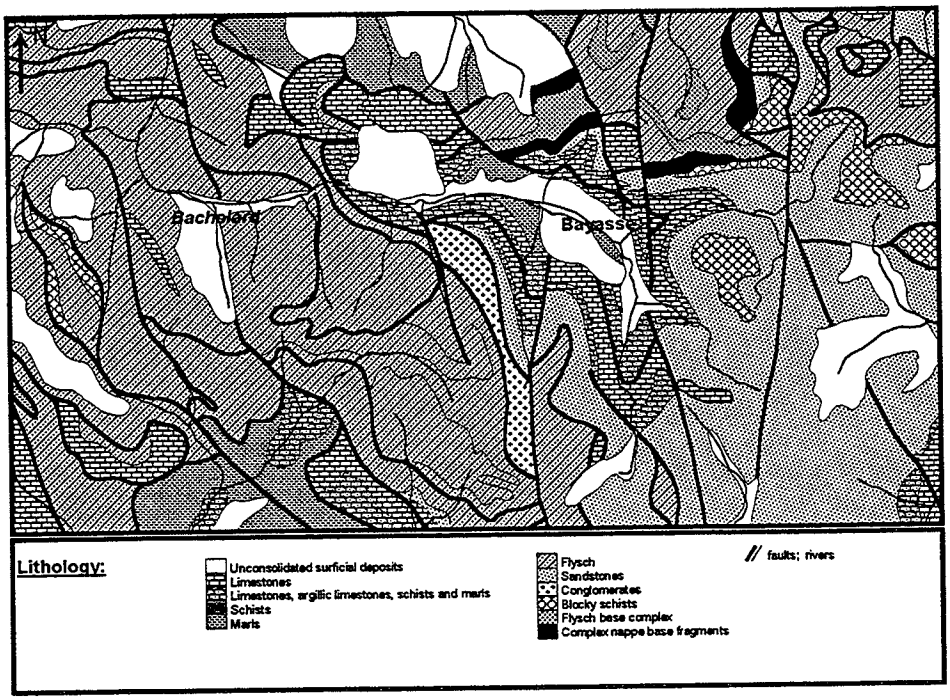

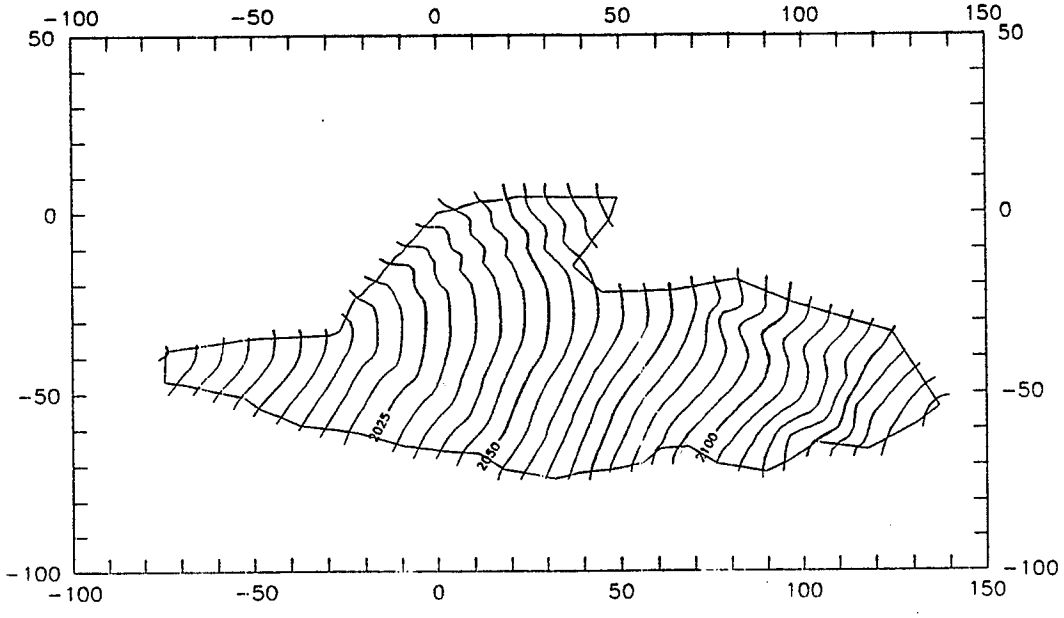

Figure 4: Contour map of the debris flow source area 'Tête du Clot des Pastres'.

action have been the main processes. At higher altitudes, periglacial conditions have significant influence on the processes at work.

The present climate in the study area has mediterranean and oceanic influences. Precipitation maxima are recorded in autumn, a secondary maximum in june. Precipitation data recorded at Fours-St. Laurent (1660m) show a mean yearly precipitation of 977mm. Orographic influences cause an increase of precipitation with height. In summer precipitation often takes the form of short-duration high-intensity rain or thunderstorms. In the Queyras, 50km to the north, the 0°C-isotherm is near 2400m. This isotherm marks the lower limit of sporadic permafrost. As most debris flow source areas are situated near this level, periglacial conditions may possibly favour the occurrence of debris flows. The influence of periglacial conditions might then be through frost action producing (coarse) debris and through frozen subsoil influencing infiltration characteristics. Local climat is strongly influenced by slope orientation. This determines the amount of rainfall coming from different directions and the amount of radiation received. According to Douguédroit & de Saintignon (1970), in the southern French Alps the differences in mean annual temperature between sun-exposed slopes and valley-floors at 2000m altitude are 3.4°C, 1.6°C and 0.2°C for respectively minimum, mean and maximum temperatures.

Debris flow source areas are usually located between 2100 and 2800m. They are often found in places with a rapid alternation of weak and resistant rocks. Hovius (1990) describes typical debris flow source areas in the Bachelard valley as spoon- or funnel-shaped concave parts of slopes. Downslope they are limited by an outcrop of resistant bedrock through which the source areas drain through a narrow channel. Slope angles within typical source areas are between 33° and 38° (also reported by Van Steijn, 1991). Drainage channels have gradients of at least 30° (Van Steijn, 1991). On the channel floors coarse, cohesionless debris has accumulated, transported by rockfall. The slopes bordering the channels consist of either solid bedrock or more or less fine-grained regolith. Vegetation consists mainly of grasses and herbs and covers less than 10% of the source area (Van Steijn, 1991). Slopes within the source areas consist of bedrock or are covered with a thin mantle of relatively fine regolith. The thickness of this material is highly variable from place to place. When dry, the surface forms a strongly cemented crust.

Debris flow deposits are found between 1700 and 2400m in this area. Debris flow tracks are usually several 100s to over 1000m long. Most of the debris flows in the study area fall in the category smallscale flows (1-10^3 m^3) as defined by Innes (1983). Of these, the larger part are 10^2-10^3 m^3). Only a few are mediumscale flows (10^3-$10^5 m^3$). Reported velocities are 1-10m/s (Van Steijn, 1988; Van Steijn et al., 1988).

THE TÊTE DU CLOT DES PASTRES DEBRIS FLOW SOURCE AREA

In one of the debris flow source areas in the Bachelard Valley detailed

measurements have been done. This site is situated at 1 km south-east of Bayasse, between 2000 and 2150 m on the west-facing slope of the Tête du Clot des Pastres (2661 m). Figure 2 a shows the location of this debris flow source area. A contour map of this source area is given in figure 4. The length of the source area is 200 m, its maximum width is about 75 m. Slope angles in the Tête du Clot des Pastres source area are 35°-38° in the main channel and over 40° on the side slopes. Figure 5 is a photograph of this source area.

Above 2055 m the Oligocene Grès d'Annot sandstones outcrop in the source area. They overlay a several metres thick limestone bank from the lower Cretaceous. Between 2025 and 2050 m marls are found which lie on top of limestones. Both are from the lower Cretaceous. Under the lowest limestone outcrops the bedrock lithology is masked by the presence of slope deposits (Fig.6).

The main drainage channel is not sharply incised, but forms a shallow, 20 m wide channel. On the floor of the channel coarse, cohesionless debris has accumulated (Fig.7). This debris is mainly supplied from the upslope sandstones by (single particle) rockfall. Individual stones are up to 2 m long, but stones of 1-25 cm dominate. Within the accumulated debris some tracks are visible which show a certain degree of sorting. The material in these tracks has probably been transported by dry grain flow; dry grain flows causing similar sorted tracks have been observed in the debris mass. Initiated by rockfall or by treading, they usually moved at a rate of few decimetres per second over a total distance of no more than several metres. The relatively easy initiation of these dry grain flows shows that the debris has accumulated at an angle only slightly less than the angle of internal friction of this cohesionless material.

Above 2090 m the main channel splits into two separate channels which gradually fade towards the upper limit of the source area. In these channels only little debris has accumulated. The side slopes bordering these channels have slope angles up to 80°-90°. In this part of the source area some vegetation is present. Vegetation may cover up to 25% of this part of the source area. Besides herbes some trees stand here (Larix decidua).

The marls in the lower part of the source area are covered with regolith, as can be seen in figure 8. This regolith contains less than 1% clay&silt, and 35-80% sand, the rest is mainly composed of small stones (< 5 cm). In dry periods, the top layer (1-2 cm) of the regolith becomes dessicated and forms a strong crust, cemented by lime. In wet periods this crust is absent and the surface may be very soft. The regolith is sensitive to erosion by overland flow, which has resulted in the formation of sharply incised gullies, especially on the slopes bordering the main channel on the north (Fig.8). The gullies have mean slope angles of 42°, whereas the side slopes of these gullies are 39°-50° and are scarred by many rills. Rills and gullies are blurred or masked at the end of spring (Fig.9 a). Evidence has been found of masses of regolith that have flowed over or at the surface into the gullies, where they have accumulated. These might be solifluction masses initiated by an increase of pore pressure caused by saturation of the regolith during the period of snowmelt and spring rainfall. In summer, heavy rainstorms produce overland flow, which makes rills and gullies deeper and sharper contoured (Fig.9b). In the northernmost gully in these marls the hydrologic monitoring unit was installed in 1991. Figures 10 shows a photograph and figure 11 a map of this gully.

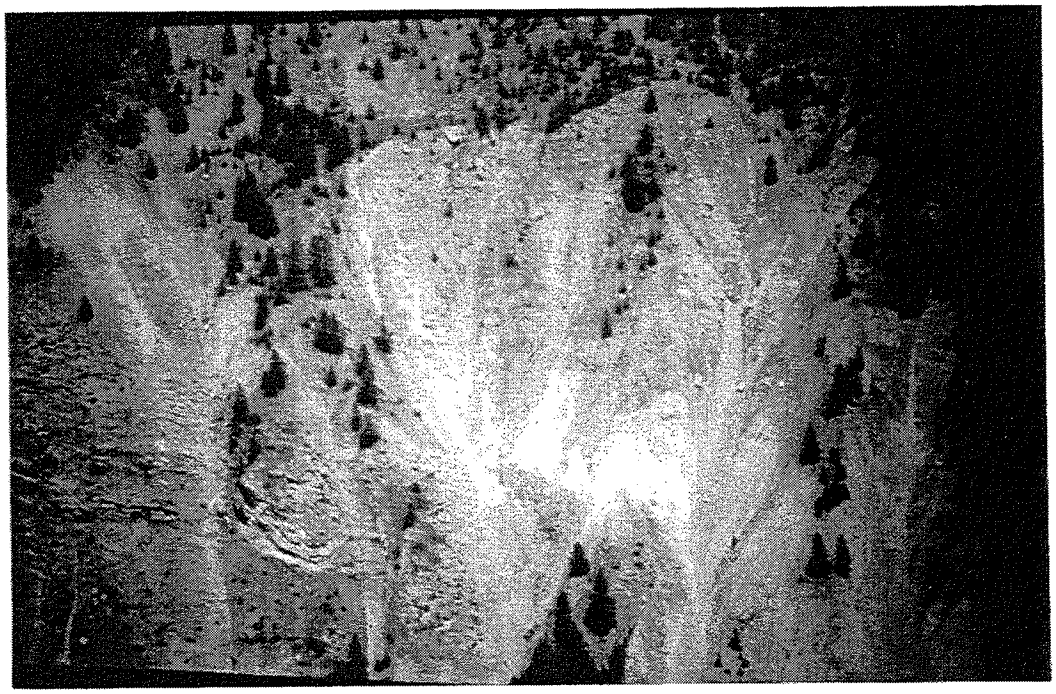

Figure 5: The debris flow source areas 'Tête du Clot des Pastres - North' and 'Tête du Clot des Pastres'.

Figure 6: The west-facing slope of the Tête du Clot des Pastres with a zone of debris flow source areas.

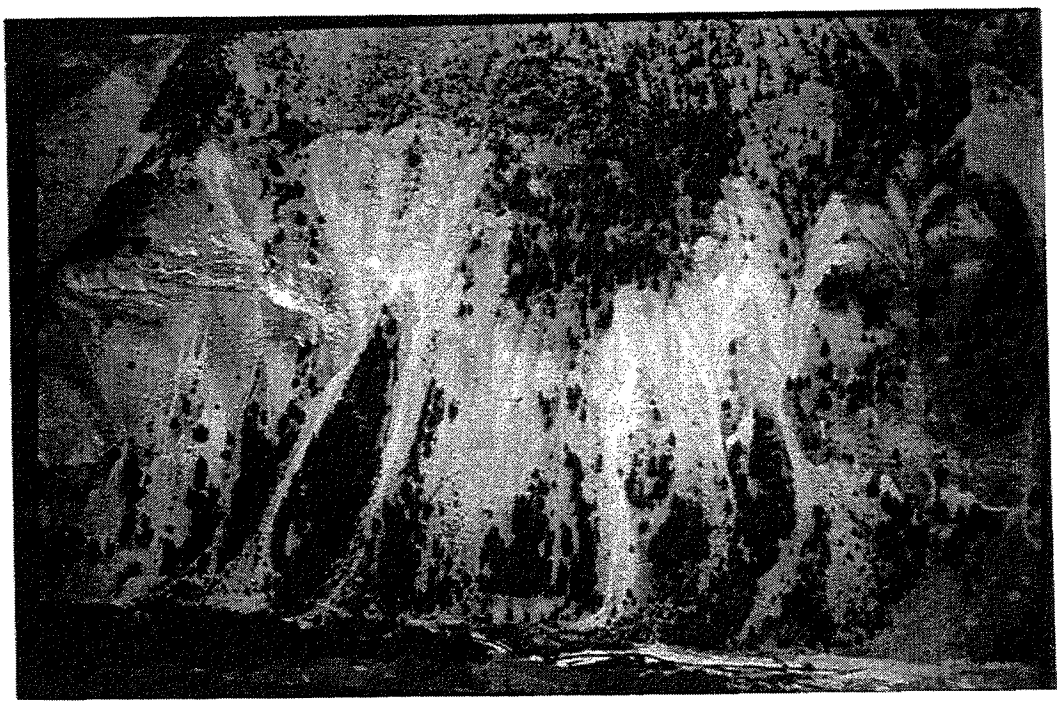

Figure 7: The main channel of the 'Tête du Clot des Pastres' debris flow source area, covered with coarse debris.

Figure 8: Marls covered with regolith in the 'Tête du Clot des Pastres' debris flow source area. In the gully on the left the hydrologic monitoring installation is visible.

a: At the end of spring (1992).

Figure 9: The surface of the regolith covering the marls in the 'Tête du Clot des Pastres' debris flow source area.

b: At the end of summer (1992).

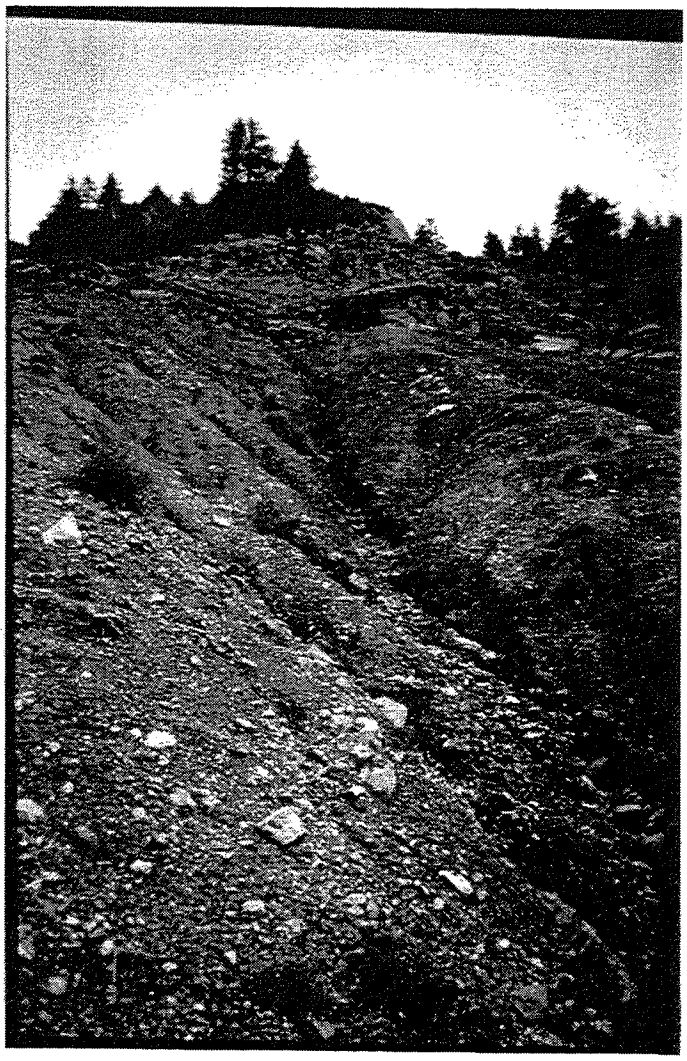

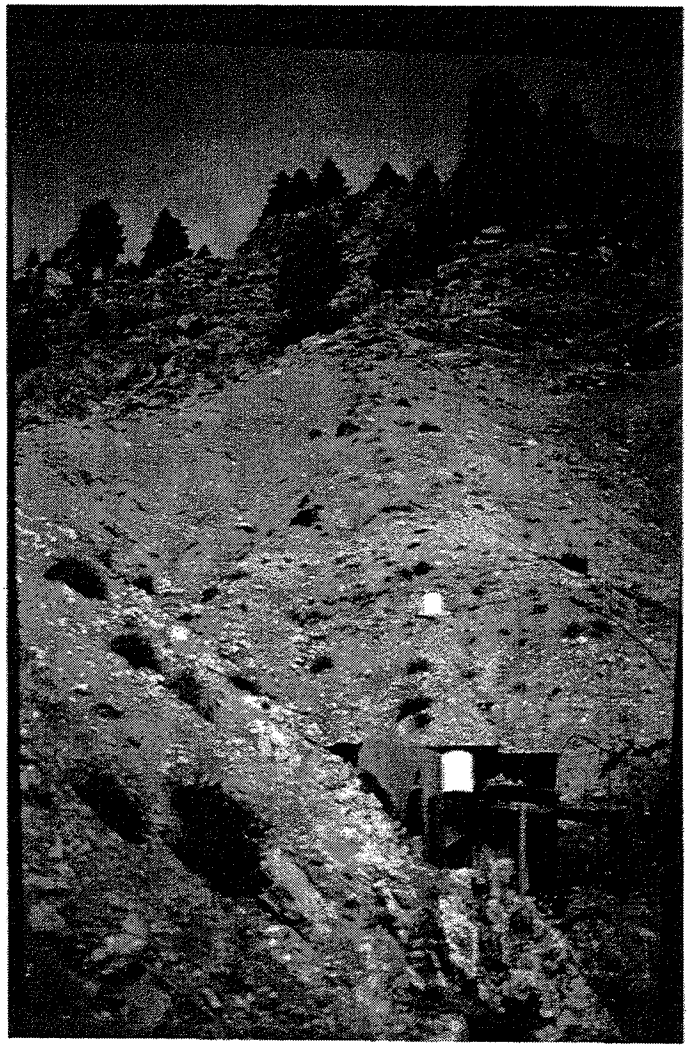

Figure 10: The monitored gully with the hydrologic monitoring unit.

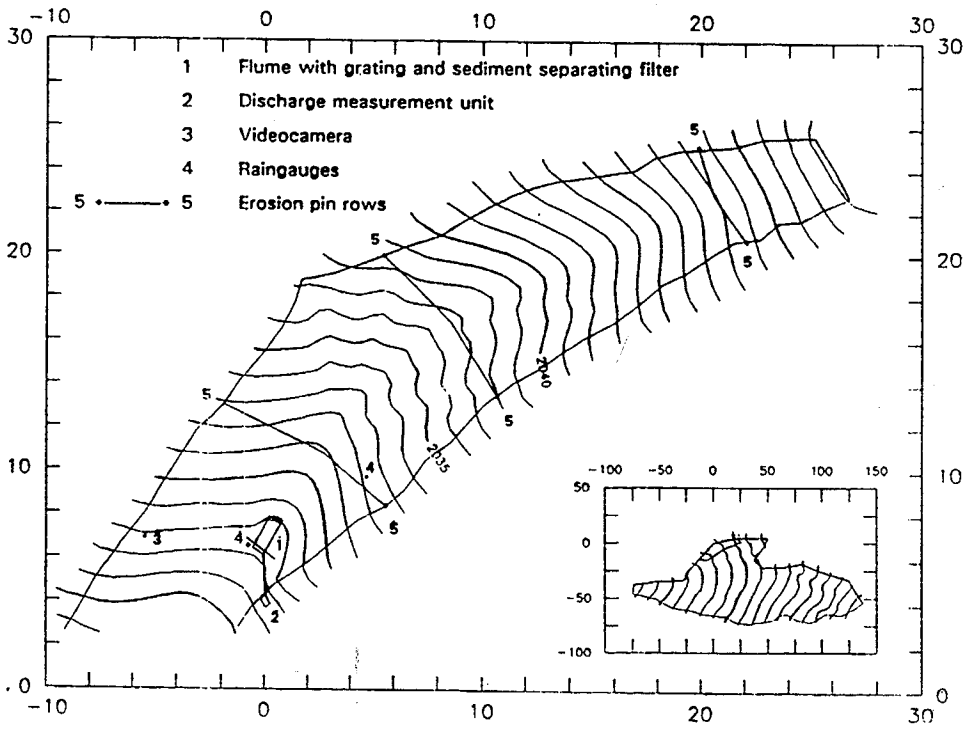

Figure 11: Map of the monitored gully in the 'Tête du Clot des Pastres' debris flow source area.

Downslope of the marls, where limestones outcrop, the source area suddenly narrows. The side slopes are steeper and the main channel is narrowed down to 6-7 m, and a thick accumulation of coarse debris (1-2 m) is found here. Beneath this narrowing debris flow deposits can be found (Fig.12 a) from 1975 m all the way down to the Bachelard river, which flows at 1820 m. The debris flow deposits found here are characterized by coarse debris (10-50 cm), filled with a finer-grained matrix. Debris flow deposits can be found as well in the source area. Here they can remain recognizable for several months after the occurrence of the debris flow, but then they become blurred by rockfall and dry grain flow action. These deposits are distinctly different from the deposits underneath the source area. Levees are less wide and high and they contain few stones > 10 cm (Fig.12 b).

OBSERVATIONS

Observations in the Tête du Clot des Pastres source area and other source areas have contributed to the understanding of processes involved in the initiation of debris flows. Changes observed in the morphology of source areas over the years and during summer have indicated which processes might be involved. These processes seem to be small-scale mass movements (like debris (flow-)slides, solifluction and rockfall) and overland flow, often containing a large amount of debris. Indications for these processes are:

- A more or less smooth surface of the relatively fine-grained regolith in the marls at the end of the snowmelt period, with some scars and cracks at the surface. This points to the occurrence of solifluction of the whole surface layer during the snowmelt period. Accumulated (solifluction) debris masses have been found on the gully floors in the regolith.

- Small scarps with a convex shaped mass beneath the scarp. In wet periods and near sources the regolith masses can fail because of high pore pressures and form small debris (flow-)slides. These mass movements may have started as slides, but the masses quickly lose consistency and after only a few cm of movement they may transform into a flowing movement.

- Rill formation and incision of the debris masses in the gully floors in the regolith show the activity of running water. As these phenomena become more pronounced in the course of summer, when high-intensity rainstorms occur, they are probably caused by overland flow during these rainstorms. Sometimes small levees are formed, pointing to the occurrence of very small debris flows. The easy entrainment of the debris on the steep slopes may be responsable for the large amount of material transported in these areas.

- Accumulations of coarse debris in the main drainage channels are mainly caused by (single particle) rockfall. Sometimes tracks of slightly sorted material within these debris accumulations can be seen. The most probable explanation for these tracks is dry grain flow.

a: Coarse deposits downslope of the debris flow source area.

Figure 12: Debris flow deposits at the 'Tête du Clot des Pastres' site.

b: Relatively fine-grained deposits in the debris flow source area.

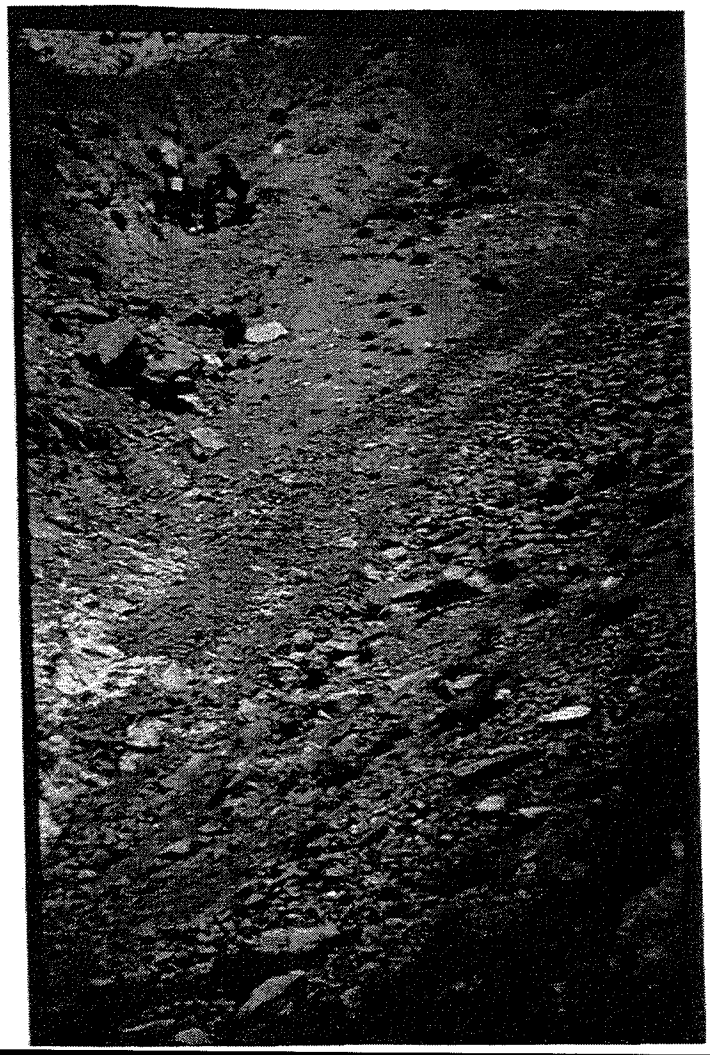

These phenomena and changes have sometimes been observed "live" in the field. Photographs taken in some areas with more or less regular intervals have also been used, especially for the more subtle changes. Video camera recordings in the Tête du Clot des Pastres source area have contributed to the understanding of the processes involved during high-intensity rainstorms. Overland flow during such rainstorms usually seemed to contain a high amount of relatively fine-grained debris. Sometimes the amount of solids in the water was high enough to call the flow a debris flow. When such a (micro-scale) debris flow occurred, the discharge would be a surge-like phenomenon. Such surges have often been observed in much larger debris flows as well (Pierson, 1980 and 1981; Costa, 1984). These phenomena have been recorded by the video camera on august 19th and 29th 1992 and on july 10th 1993.

'New' debris flow deposits have been found several times since 1991. Especially the extreme meteorological conditions of late september 1992 in south-east France have initiated many debris flows all over the study area. Over twenty recent debris flow tracks were found only two weeks later.

MATERIAL PROPERTIES

PROPERTIES OF THE FINE-GRAINED REGOLITH

Figure 13 represents the grain size distributions of samples taken from the regolith in the source areas of Tête du Clot des Pastres and at Pra Bouréou North (Fig.2). The distributions are given for grain sizes 53-2000 µm. As can be seen, the samples contain very little clay/silt. The amount of clay+silt is usually <1%. Sand occupies 35-60% of the regolith, the rest consists of coarser material, mainly small stones up to several centimetres. The very small fraction of clay+silt is remarkable, as this grain size fraction is usually thought to play an important role in debris flows. The regolith samples from Pra Bouréou North and Tête du Clot des Pastres have about the same size distribution. This is not surprising, as the parent material is the same for both debris flow source areas.

LOCATION	NUMBER OF SAMPLES	DRY BULK DENSITY (KG/M ^{3})				SOLIDS DENSITY (KG/M ^{3})				POROSITY			
		x	σ	min	max	x	σ	min	max	x	σ	min	max
Tête du Clot des Pastres 1991, all data	41	1644	155	1374	1999	2506	277	2099	3099	0.342	0.054	0.173	0.448
Tête du Clot des Pastres 1992, all data	111									0.231	0.042	0.148	0.517
Tête du Clot des Pastres 1992,dry period	18									0.234	0.024	0.194	0.292
Tête du Clot des Pastres 1992,wet period	93									0.230	0.045	0.148	0.517
Combal du Menon 1992, all data	12									0.280	0.028	0.235	0.340

Table 1: Density and porosity characteristics of fine-grained regolith material.

The density, porosity and field water content of the fine-grained regolith has been determined by means of pF-samples. Table 1 shows the result for dry bulk density, solids density and porosity of the regolith in the debris flow source areas of Tête du Clot des Pastres and Combal du Menon. The Combal du Menon site is situated at 1800 m altitude in the Vallon du Lau, 4 km south-east of Jausiers (Fig.2 a). The regolith porosities of these two debris flow source areas probably do not differ significantly.

A remarkable difference in porosity has been found between the Tête du Clot des Pastres samples taken in 1991 and in 1992. The cause for the difference might be the swelling/shrinking behaviour of the material that was sometimes observed. When a dry sample was wetted, the sample would occupy more than the total volume of the pF-ring, whereas a sample taken in wet material occupied exactly the volume enclosed by the pF-ring. This means that more water can be contained in the initially dry sample, resulting in a higher calculated porosity than for an initially wet sample, if a constant volume is assumed. Three samples taken in wetted material (from rainfall simulations) in 1991 showed the same difference. On the other hand, initially dry samples taken in 1992 in the dry period after a prolonged wet period did not show significant different porosities from those taken in the wet period. A possible explanation for this might be that after a prolonged wet period the regolith needs a long time of recovery before 'dry' conditions are obtained. A single rainstorm in a dry period does not seem to have a long-term effect on the regolith properties.

LOCATION	NUMBER OF SAMPLES	FIELD WATER CONTENT			
		x	σ	min	max
Tête du Clot des Pastres 1991, dry surface	37	0.077	0.030	0.006	0.165
Tête du Clot des Pastres 1991, wet surface	3	0.161	0.005	0.154	0.166
Tête du Clot des Pastres 1992, all data	112	0.080	0.043	0.009	0.336
Tête du Clot des Pastres 1992, dry period	18	0.037	0.018	0.009	0.087
Tête du Clot des Pastres 1992, wet period	94	0.088	0.042	0.015	0.336
Combal du Menon 1992, all data	12	0.060	0.017	0.038	0.087

Table 2 : Field water content of regolith material.

Table 2 contains the results of the water content measurements for field situations. Samples of regolith which have been taken immediately after rainfall simulations have a significantly higher water content than the other samples. The small range of water contents measured in these samples, even though it is only based on three samples, is remarkable. Samples taken in a wet period in 1992 in the Tête du Clot des Pastres area have a mean water content of 0.088, over twice as much as those taken in the dry period (0.037).

Figure 14 shows pF-curves for material from Tête du Clot des Pastres and Combal du Menon. Both materials lose most of their water between saturation and field capacity (pF ≈ 2.5). At field capacity, the water content is slightly higher than the measured field water contents. This can be explained by the presence of material from the surface of the regolith in the field water content samples. In dry periods, this layer (1-2 cm) is dessicated, protecting the underlying material against evaporation. The slight differences between the samples from the Tête du Clot des Pastres area and the Combal du Menon area are not statistically significant, but may still be relevant for field conditions and hydrologic response.

Regolith thickness in the gully and its side slopes directly south of the gully with the hydrologic monitoring unit in the Tête du Clot des Pastres source area showed a mean regolith thickness of 0.44 m. Maximum measured regolith thickness was about 1.0 m. These values are believed to be valid as well for the gully where the hydrologic monitoring unit has been placed. The regolith thickness is significantly less on the gully floor than on the side slopes.

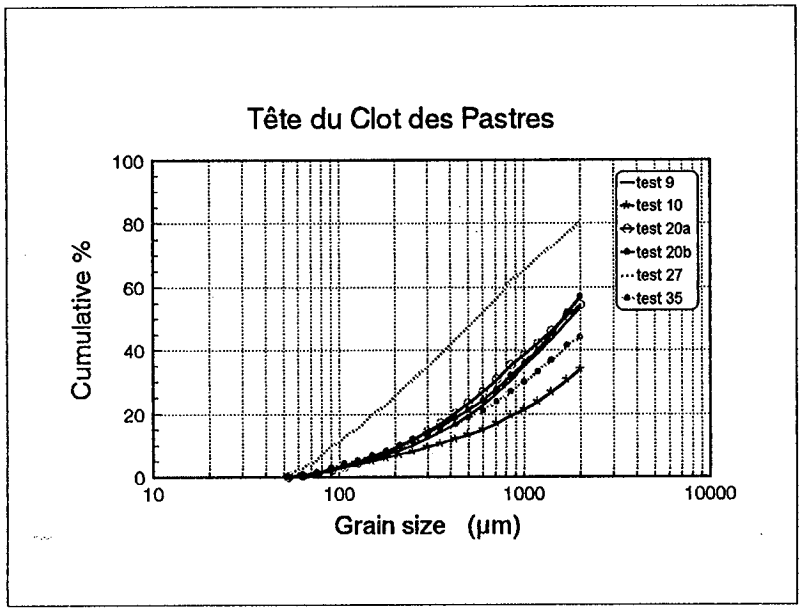

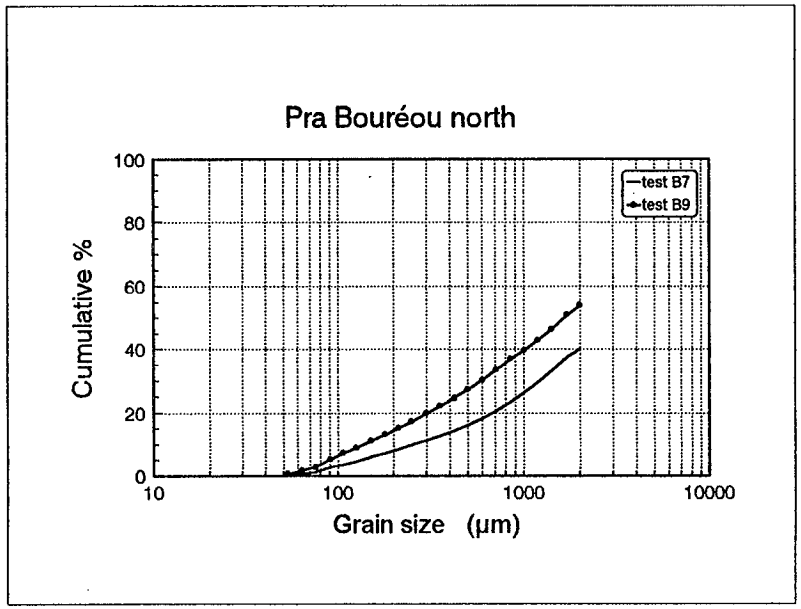

Figure 13: Grain size distribution of regolith material from debris flow source areas

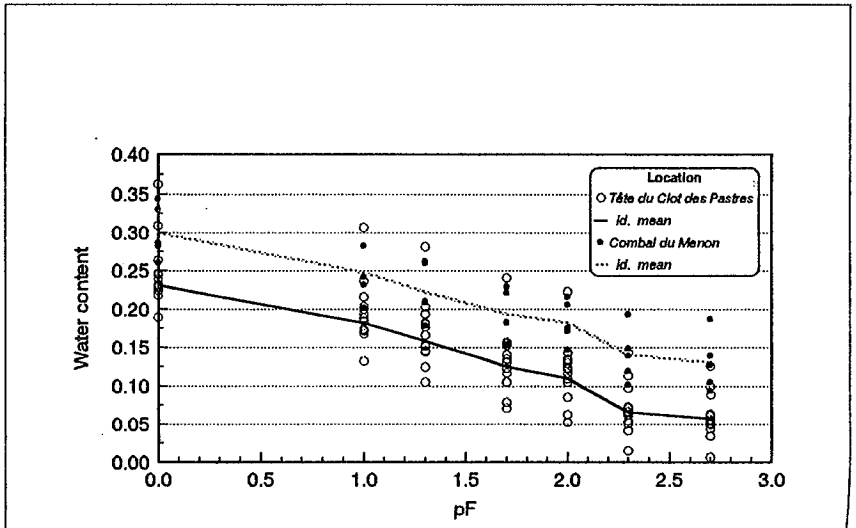

Figure 14: pF-curves of regolith material from debris flow source areas.

Porosity measurements of coarse debris revealed a mean porosity of 0.44 (table 3). Not surprisingly, porosity depends on degree of packing: densely packed debris had a mean porosity of 0.43, whereas for loosely packed debris this was 0.48. Degree of sorting has even more influence: the mean porosity increased from 0.37 for very poorly sorted debris to 0.48 for well sorted debris. The difference in porosity for different grain sizes is very small. It is probably caused by the effect of sorting and packing, which could not be isolated from the other parameters.

SAMPLE TYPE	NUMBER OF SAMPLES	POROSITY			
		x	σ	min	max
PACKING					
dense	67	0.43	0.04	0.33	0.50
loose	77	0.48	0.04	0.40	0.59
MEAN GRAIN SIZE					
< 25 mm (fine)	52	0.43	0.05	0.33	0.50
≥30 mm (coarse)	102	0.46	0.04	0.34	0.59
SORTING					
very poor	9	0.37	0.04	0.33	0.43
poor	53	0.42	0.04	0.34	0.50
quite poor	14	0.44	0.02	0.42	0.49
good	78	0.48	0.03	0.40	0.59

Table 3 : Porosity of coarse, matrixless debris.

Table 4 contains the results of the measurements of the dynamic angle of internal friction ϕ_d for coarse debris. The values range from 36.0° for limestone debris to 38.7° for a mixture of rock types (mainly sandstone and limestone with some marls). The differences between the mean values for the 5 rock types are not statistically significant (95%). Yet, as the debris flow initiation model is very sensitive to the internal friction value (Fig.15), the small differences were related to other parameters of the debris that have been measured. These are mean stone size (a-axis length), mean stone shape (represented by the ratio b-axis length to a-axis length and ratio c-axis to a-axis) and degree of sorting (represented by ratio standard deviation to mean, for both stone volume and a-axis length). Sorting, based on stone volume, explains most of the variation of ϕ_d: 71%. The large part of the variation explained by sorting can lead to two different conclusions: either sorting depends on rock rock type and the variation explained is not directly through sorting but through rock type; or sorting is the factor causing the differences between the friction angle values. The two rock-mix-types probably hold the key to the interpretation of the data. Their rock type composition is about the same, but they do differ in their degree of sorting and in their internal friction angles. This leads to the conclusion that the second explanation proposed must be the right one.

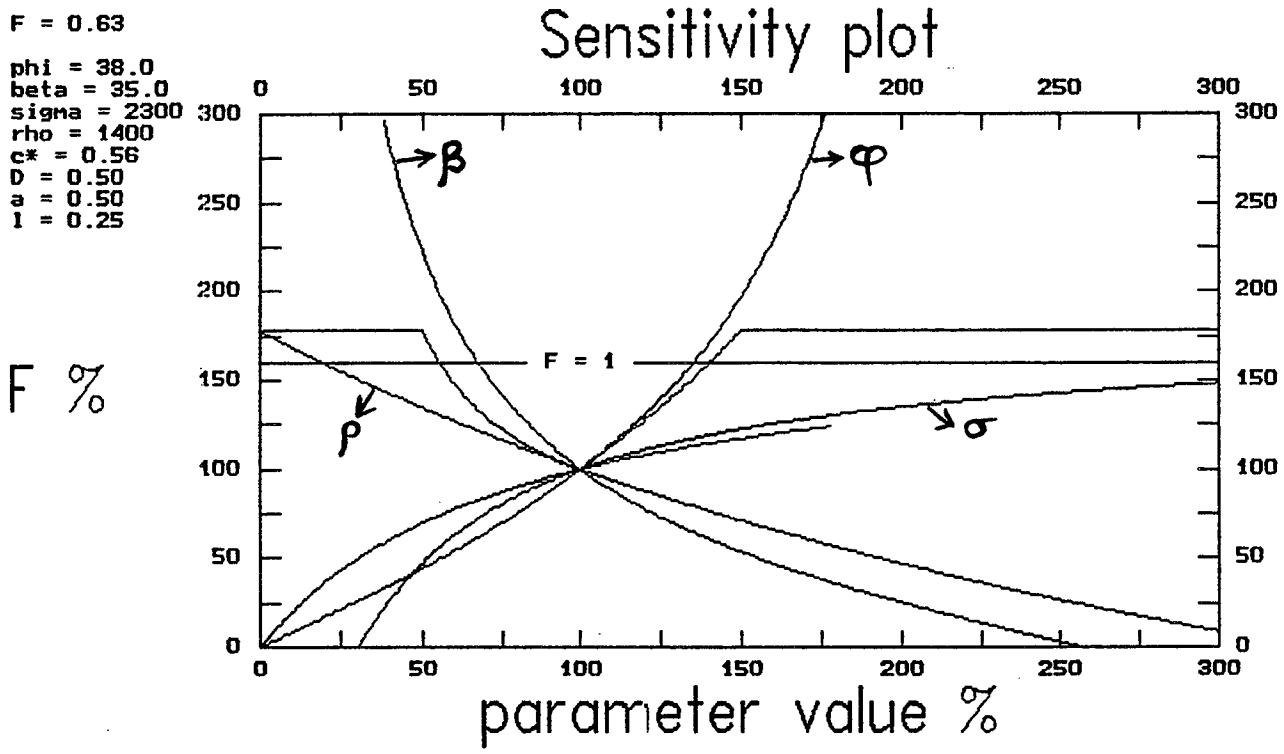

Figure 15: Sensitivity analysis of the Takahashi debris flow initiation model.

DEBRIS TYPE	NUMBER OF SAMPLES	INTERNAL FRICTION ANGLE				MEAN DIMENSION	MEAN SHAPE		MEAN SORTING (σ/mean)	
		x	σ	min	max	a-axis length	b/a	c/a	volume	a-axis
Limestone	50/100	36.0	1.3	34	40	51	0.66	0.39	1.83	0.57
Sandstone	50/100	37.7	2.2	33	43	70	0.62	0.40	2.98	0.66
Flysch	50/100	38.8	1.8	34	42	95	0.56	0.25	2.88	0.86
Mixture 1	50/100	36.6	1.8	31	40	79	0.67	0.38	2.72	0.78
Mixture 2	50/100	38.7	2.0	36	43	65	0.67	0.45	4.51	0.84
VARIATION IN INTERNAL FRICTION EXPLAINED BY VARIABLE						21 %	17 %	1 %	71 %	55 %

Table 4: Dynamic angle of internal friction of coarse, matrixless, cohesionless debris.

RAINFALL

Although rainfall is recorded at Fours-St. Laurent (Fig.3), additional rainfall measurements have been done. The data necessary for infiltration and runoff modelling are short-duration rainfall intensities and rainfall duration, which cannot be derived from the daily totals measured at Fours-St. Laurent. The raingauges connected to the hydrologic monitoring unit in the Tête du Clot des Pastres debris flow source area were installed in 1991. In that year they functioned in the period 14 june - 16 september. In 1992 registrations were made in the period 15 june - 5 october. Additional data from a hand-held raingauge, which was regularly checked, have been used for a check of the automatic raingauges.

Even though the two automatic raingauges were installed quite close to one another (Fig.11), they did not register the same amount of rainfall. In figure 16 the registrations made by both raingauges are compared. Using the data from the hand-held raingauge, it was decided in 1991 to use the mean values of both automatic raingauges, whereas in 1992 only the data obtained from the raingauge placed on a ridge (PLU2) were used. That year, a stone had hit the other raingauge (PLU1) a few days after registration had started. As can be seen in figure 16 b, the initially nearly equal registrations suddenly changed. During the rest of the period PLU1 registrated about 10% less rainfall than PLU2.

Table 5 and figure 17 present some of the data that were obtained from the raingauges. The maximum amount of rainfall in one day that has been recorded was over 80 mm, on september 22nd 1992. Maximum rainfall intensity occurred on july 12th 1991: the 5-minute mean intensity i_5 was 130 mm/h. This occurred in a short-duration thunderstorm.

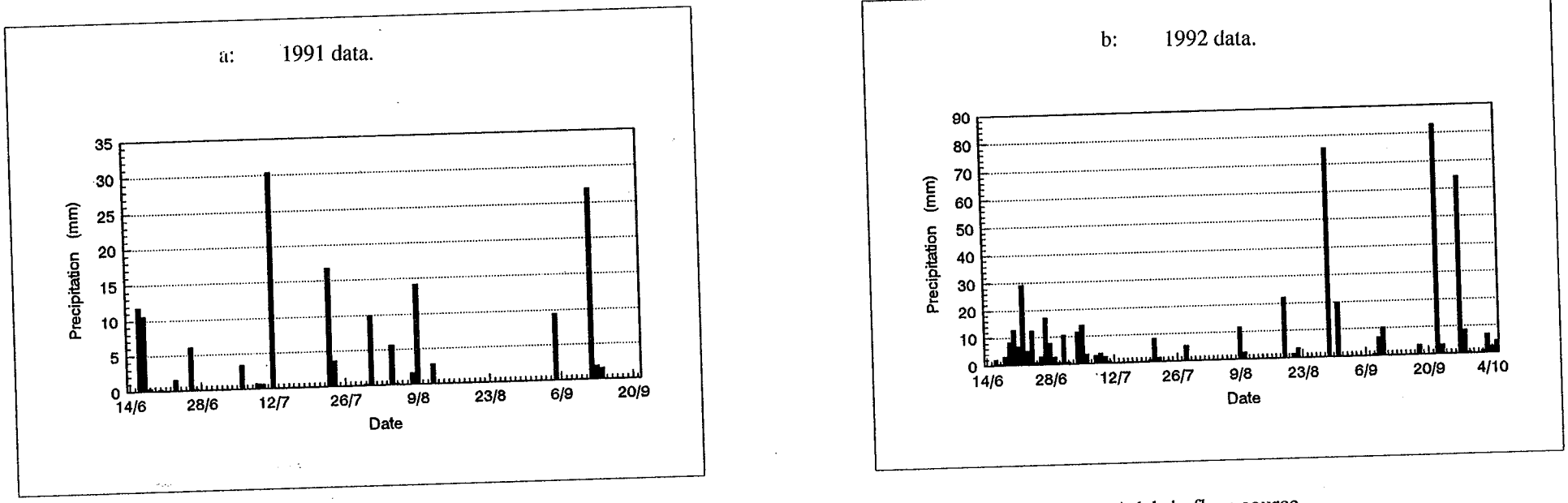

Figure 17: Daily rainfall recorded by the raingauges in the 'Tête du Clot des Pastres' debris flow source area.

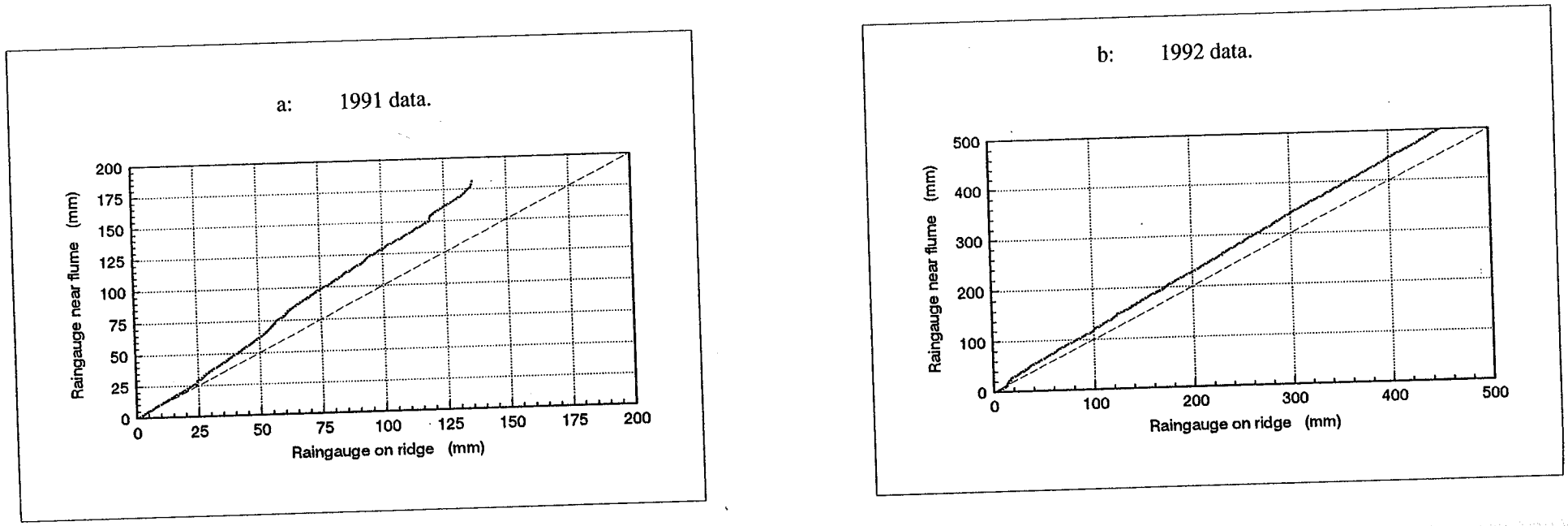

YEAR	DATE	STARTTIME	DURATION	TOTAL AMOUNT OF RAIN(mm)	MAXIMUM RAINFALL INTENSITIES (mm/hr)					
					i_1	i_3	i_5	i_{10}	i_{15}	i_{30}
	16/6	20:23	1:22	4.0	18.0	14.0	12.0	9.0	8.4	
	17/6	2:42	3:00	8.2	12.0	10.0	9.6	7.8	6.8	
	26/6	17:11	1:06	4.4	30.0	24.0	18.0	11.4	8.0	
	12/7	14:07	1:46	30.1	138.0	132.0	128.4	109.2	85.2	
	23/7	14:32	2:43	10.4	102.0	52.0	33.6	19.8	20.8	
	23/7	22:39	1:04	4.6	12.0	12.0	9.6	9.6	8.8	
1991	31/7	11:32	0:55	6.0	24.0	20.0	16.8	13.8	12.4	
	./8	17:31	1:05	5.1	24.0	22.0	19.2	11.4	11.6	
	9/8	5:03	0:38	9.4	96.0	84.0	79.2	51.0	35.6	
	5/9	16:09	1:53	9.3	24.0	12.0	12.0	9.6	9.6	
	12/9	4:37	3:36	9.1	18.0	16.0	14.4	12.6	11.2	
	12/9	13:59	1:46	7.8	24.0	20.0	16.8	13.2	11.2	
	19/8	17:37	1:18	22.0	95.4	90.8	76.3	54.5	50.0	40.0
	29/8	12:47	1:01	17.3	54.5	40.9	35.4	28.6	23.6	20.0
	29/8	13:55	0:21	3.4	54.5	45.4	30.0	17.7	12.7	
	29/8	14:19	0:28	5.0	40.9	27.3	21.8	16.4	15.4	
	29/8	15.44	0:28	5.7	40.9	27.3	21.8	16.4	15.4	
	29/8	16:18	0:47	11.4	40.9	36.3	30.0	24.5	22.7	17.3
1992	29/8	17:11	1:18	12.3	40.9	31.8	30.0	24.5	20.0	15.4
	29/8	18:36	0:29	3.9	27.3	22.7	19.1	13.6	11.8	
	9/9	13:35	0:30	6.1	68.1	54.5	43.6	30.0	22.7	12.3
	22/9	11:52	0:37	9.5	68.1	63.6	46.3	31.3	27.3	17.7
	22/9	13:06	1:33	19.3	68.1	59.0	49.1	32.7	29.1	25.4
	22/9	16:05	4:49	40.7	40.9	31.8	30.0	27.3	24.5	17.7
	27/9	18:01	0:52	16.6	81.8	54.5	49.1	45.0	34.5	21.3

Table 5: Some precipitation events in the Tête du Clot des Pastres debris flow source area.

1991 was a normal, dry summer. In 1992 the monitoring period started with several weeks of cool and rainy weather. Rainfall usually came down as long-duration low-intensity rainfall. Figure 17 b shows that the total amount of rainfall in these weeks was high. At the meteorological station of Embrun, 30 km north-west of the study area, records of number-of-days-with-rainfall and lack-of-sunshine in june were established, but total amount of rainfall did not beat the previous record.

In summer, most precipitation in the study area usually falls as short-duration high-intensity rainstorms. Figure 18 gives the minute-to-minute rainfall intensity course of some of these rainstorms, that occurred mainly in july and august. For comparison, some other rainfall events are shown as well. The rainstorms of july 12th and august 9th 1991 and august 19th or 29th 1992 have initiated debris flows from the Tête du Clot des Pastres source area. Possibly the same has happened on september 22nd or 27th 1992. Usually these rainstorms show a quick rise to peak intensity and a more gradual decline of rainfall intensity after peak intensity has been reached.

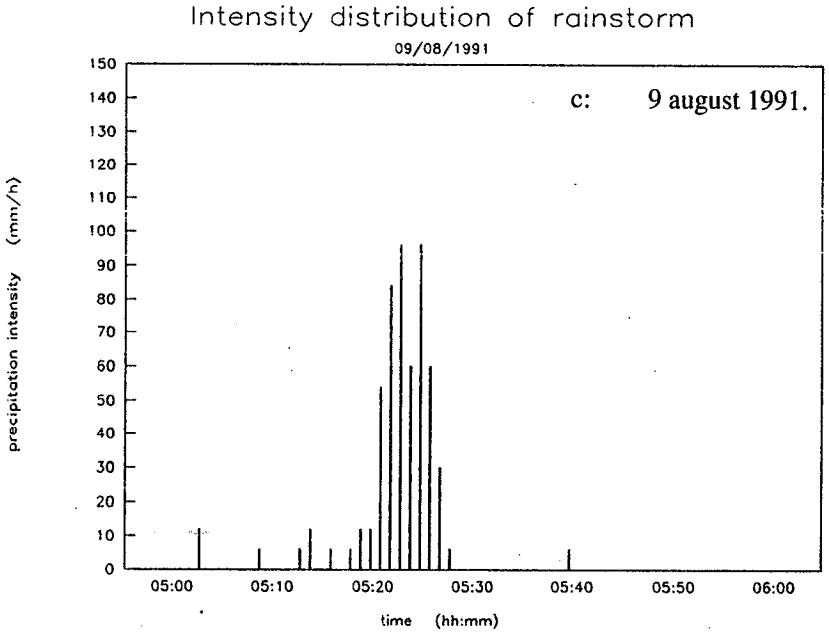
Intensity distribution of rainstorm
09/08/1991
c: 9 august 1991.
precipitation intensity (mm/h)
time (hh:mm)
05:00
05:10
05:20
05:30
05:40
05:50
06:00

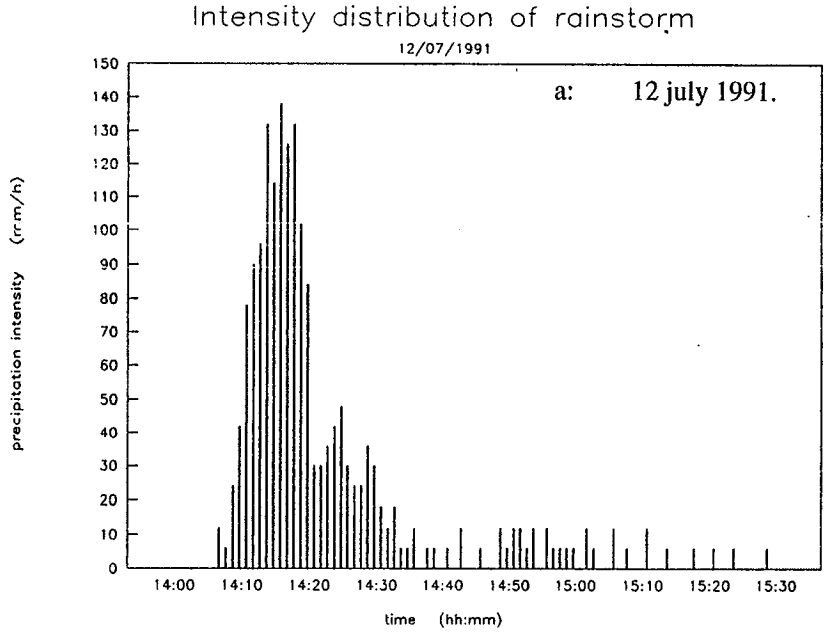
Intensity distribution of rainstorm
12/07/1991
a: 12 july 1991.
precipitation intensity (mm/h)
time (hh:mm)
14:00
14:10
14:20
14:30
14:40
14:50
15:00
15:10
15:20
15:30

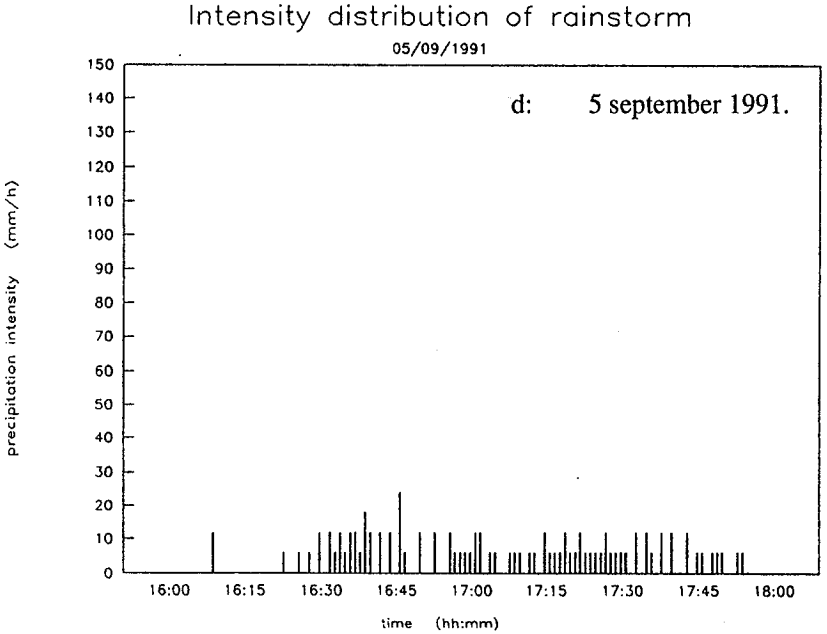
Intensity distribution of rainstorm
05/09/1991
d: 5 september 1991.
precipitation intensity (mm/h)
time (hh:mm)
16:00
16:15
16:30
16:45
17:00
17:15
17:30
17:45
18:00

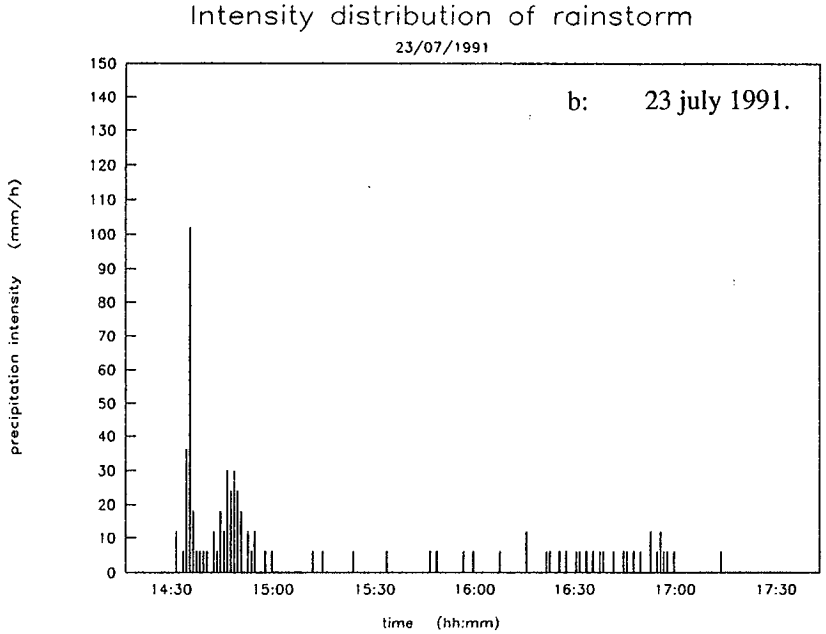
Intensity distribution of rainstorm
23/07/1991
b: 23 july 1991.
precipitation intensity (mm/h)
time (hh:mm)
14:30
15:00
15:30
16:00
16:30
17:00
17:30

Figure 18: Rainfall intensity course of rainfall events in the 'Tête du Clot des Pastres' debris flow source

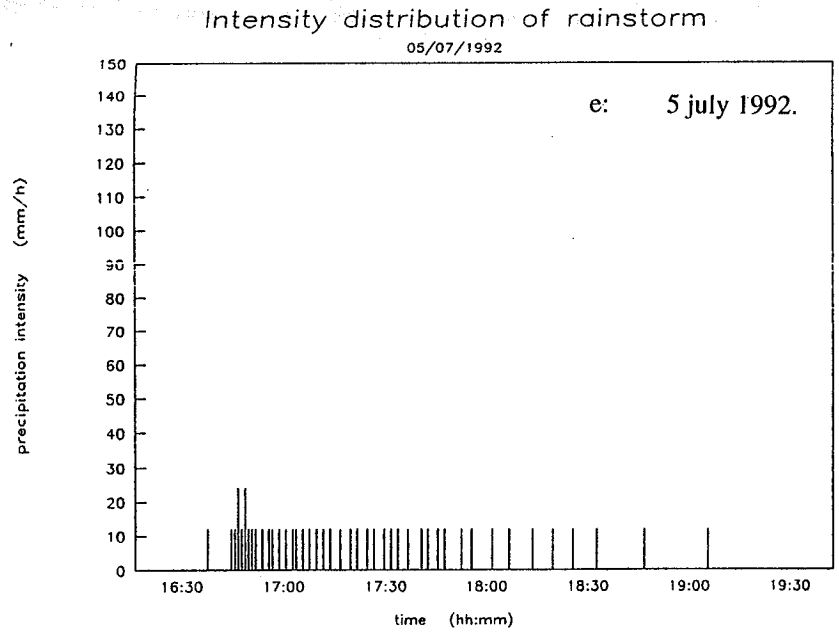

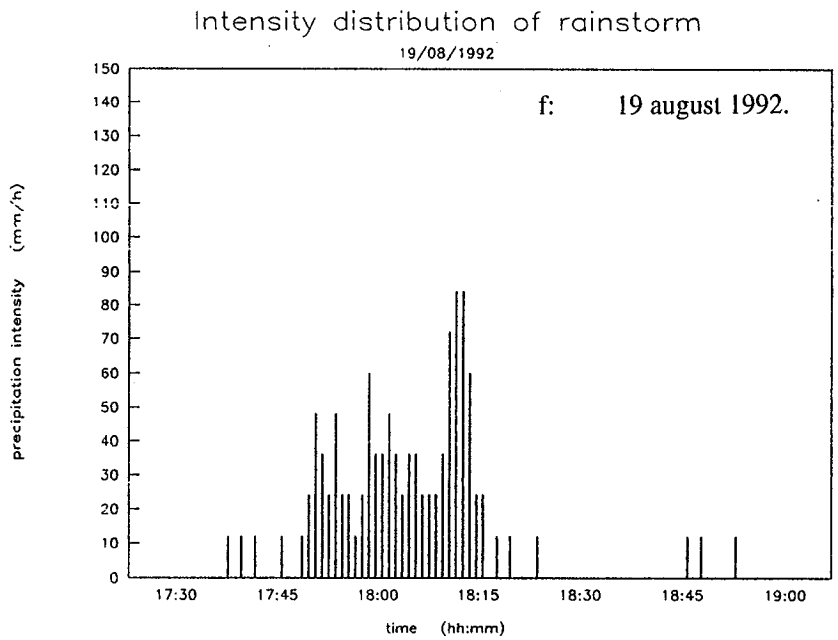

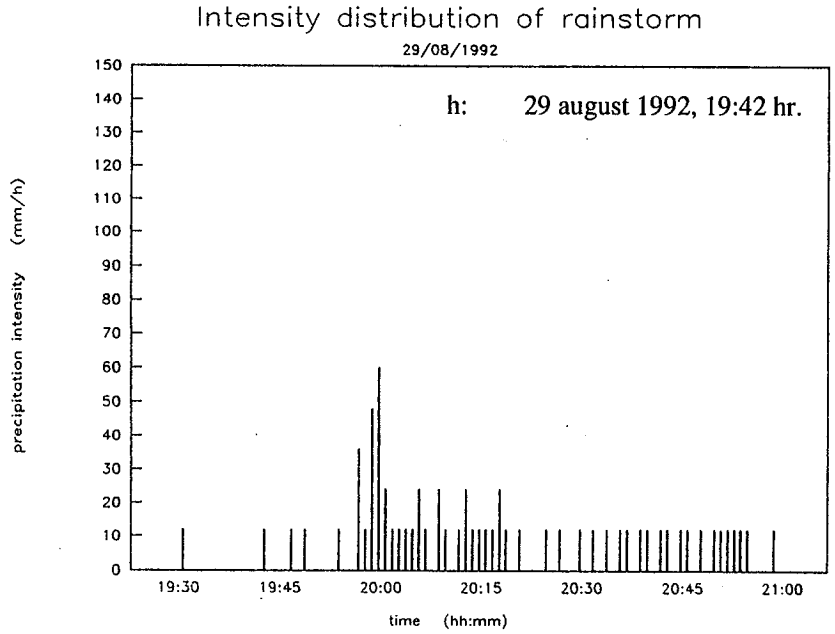

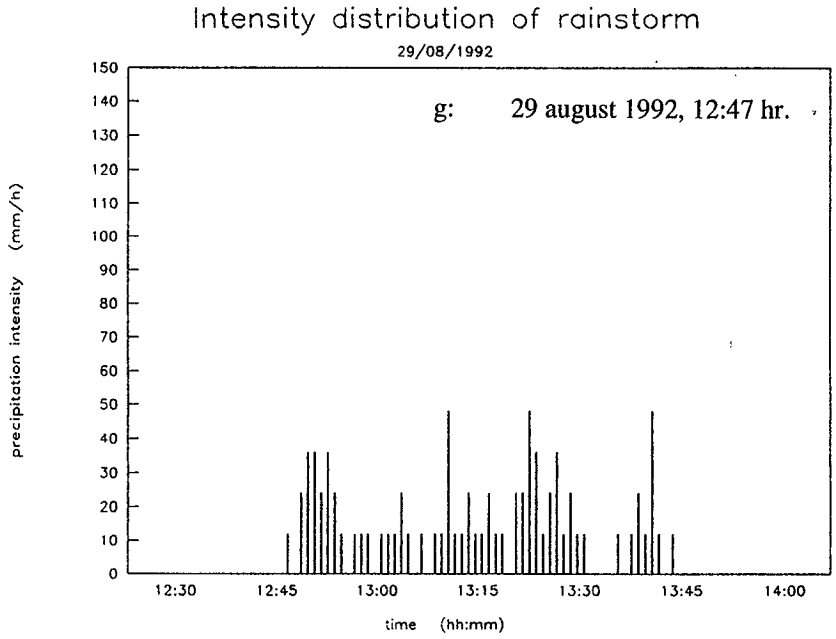

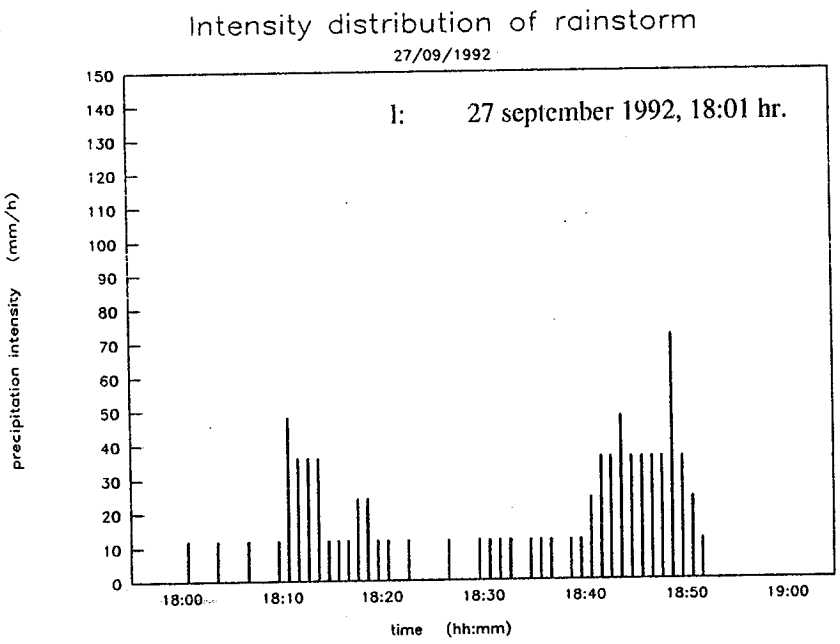
Intensity distribution of rainstorm
27/09/1992
l: 27 september 1992, 18:01 hr.
precipitation intensity (mm/h)
time (hh:mm)
18:00
18:10
18:20
18:30
18:40
18:50
19:00

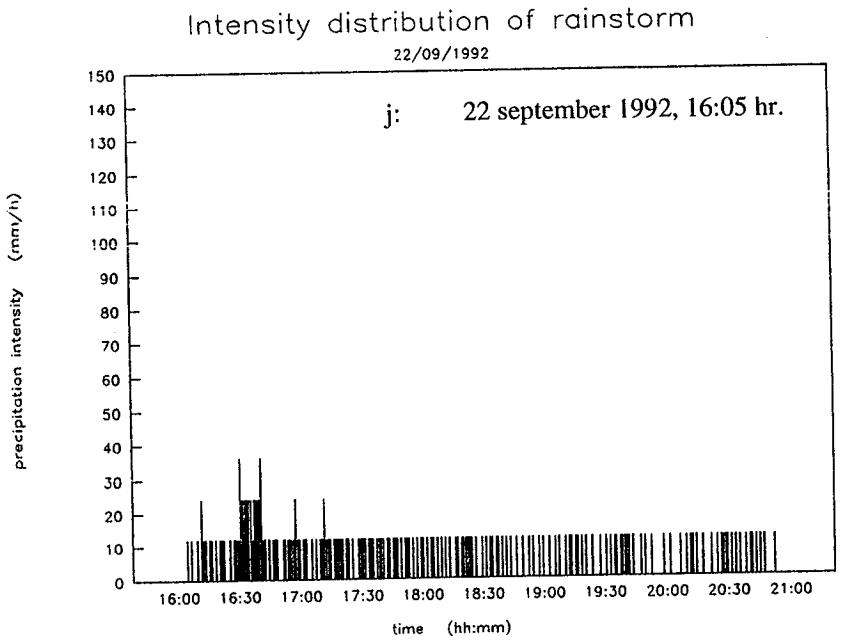
Intensity distribution of rainstorm
22/09/1992
j: 22 september 1992, 16:05 hr.
precipitation intensity (mm/h)
time (hh:mm)
16:00
16:30
17:00
17:30
18:00
18:30
19:00
19:30
20:00
20:30
21:00

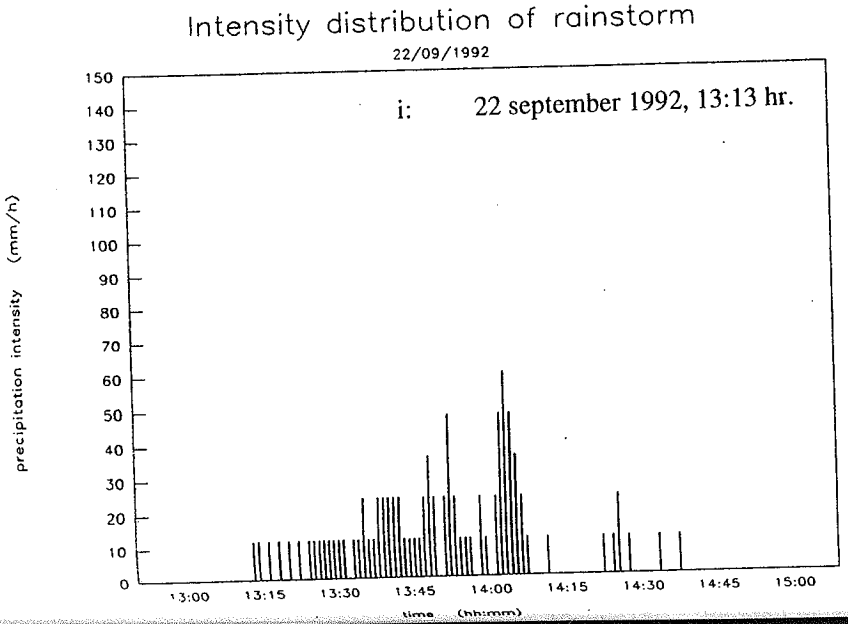
Intensity distribution of rainstorm
22/09/1992
i: 22 september 1992, 13:13 hr.
precipitation intensity (mm/h)
time (hh:mm)
13:00
13:15
13:30
13:45
14:00
14:15
14:30
14:45
15:00

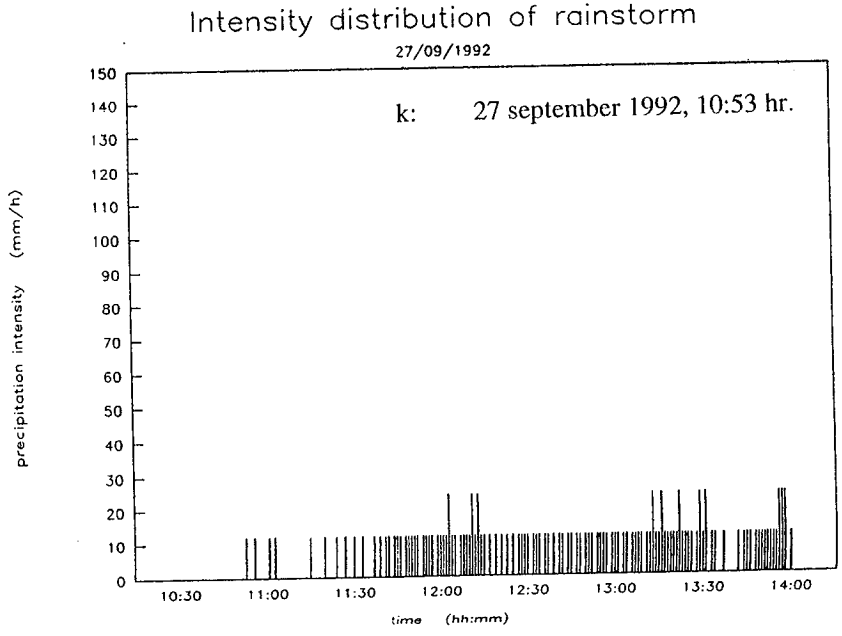
Intensity distribution of rainstorm
27/09/1992
k: 27 september 1992, 10:53 hr.
precipitation intensity (mm/h)
time (hh:mm)
10:30
11:00
11:30
12:00
12:30
13:00
13:30
14:00

The most severe thunderstorm took place in the afternoon of july 12th 1991. A total amount of 30.1 mm of rainfall fell in just over one hour. The main part of this, 26.5 mm fell during the first half hour. After the start of the event at 14:06 hr the rainfall intensity quickly increased and in the 7th minute reached 100 mm/h. The peak intensity of nearly 140 mm/h was reached in the 9th minute, at 14:15 hr. Even the maximum 5-minute rainfall intensity, i_5, was nearly 130 mm/h. The rainstorm must have been a very local event: a raingauge 1 km further to the south-west at the other side of the valley, in the debris flow source area Pra Bouréou South, had caught no more than 5 mm of rainfall. That same year two other rainfall events reached 1-minute rainfall intensities of about 100 mm/h. This happened on july 23rd and august 9th.

EROSION

Three rows of erosion pins were installed in the Tête du Clot des Pastres debris flow source area in july 1992. The pin-rows were all in the gully monitored by the hydrologic monitoring unit, upslope of the unit. The location of the pin-rows is shown on the map of figure 11. The pins were measured on july 24th and october 4th 1992 and on may 29th 1993. Figure 19 shows the surface level change along the three rows in the late summer period of 1992: july - october. The pin numbering starts at the northernmost situated pin of each row. As can be seen, most erosion took place in the gully (center of the rows). Some rills also showed much erosion. Row three does not show a pronounced erosion of the gully. This is because the row is located at about 5 metres from the top of the catchment, where there is no deeply incised gully, but only a slightly plan-concave slope. The increased erosional force of the waterflow, caused by its concentration in rills and gullies, is clearly shown by these graphs. Qualitatively, this had already been observed during several visits to the field.

Mean erosion measured from the 51 pins in the 72-day period is 15.5 mm. If the total amount of erosion in autumn, winter and spring would be about the same amount (lesser erosion rates), mean yearly erosion could be in the order of 3 cm.

In may 1993 some of the erosion pins had disappeared. Many pins had been displaced and pointed downslope. This is probably the result of solifluction activity in the snowmelt period.

GEODETIC SURVEY

The geodetic survey of two debris flow source areas has resulted in the production of digital terrain models (DTM's) of these areas. Contour maps were made based on these DTM's. The source areas concerned are Tête du Clot des Pastres and Pra Bouréou South; a contour map of Tête du Clot des Pastres is presented in figure 4. The monitored gully within the Tête du Clot des Pastres source area has been surveyed more detailedly, as this should result in a DTM which was to be used for hydrologic simulations. The contour map of this gully is given in figure 11.

RAINFALL SIMULATIONS

In 1991 168 rainfall simulations have been done with rainfall intensities 35-290 (±3%) mm/h. The error in the rainfall intensity is probably >3% at the edges of the testplot, but may be <1% in the center of the plot. After initial testing of the practicability of the method, the often used criterion of 40% ponding at the surface as the start of runoff was replaced by the moment that continuous runoff was observed. The 40% ponding criterion was not workable on the steep (35°-53°) slopes.

Initial simulations were done on slopes of 30°-40° with rainfall intensities of about 135 mm/h. At this intensity, a simulation of ±15 minutes gives a rainfall depth of ±30 mm. These simulations were mainly done to see what happened during simulations. Observations made during these simulations are:

The initially crusted surface, cemented by lime, quickly softened after the start of a simulation.

Splash occurred and could transport particles. Raindrop impact could move particles of up to ±10 mm over some distance.

Ponding usually occurred within one minute after the start of the simulation. Forced by the steep slopes, runoff starts very soon after the start of ponding.

Runoff quickly concentrated in microrills of only a few mm wide and deep. The concentration of the water causes an increase in mean flow velocity.

Splash and runoff gradually smoothed the surface. Micro-scale relief features disappeared as depressions were filled with material transported from upslope.

After a few minutes the top layer of the regolith had softened so much that the material might fail and a microscale mass movement occurred. These were usually < 100 cm^2 and only a few cm deep. Moving downslope, they quickly disintegrated and, if concentrated in a rill, might form a debris flow which could continue its way a few metres outside of the testplot.

When rainfall was continued, the process dynamics at the surface decreased. After some time runoff reached a constant discharge.

After a simulation, the wetting front usually was less than 10 cm deep. With a rainfall depth of 30 mm this would mean an increase of volumetric water content of at least 30%.

CONSTANT RUNOFF TESTS

Hydraulic conductivity K could easily be calculated when the rainfall simulations were continued until a constant runoff discharge was obtained. The difference between rainfall intensity and runoff intensity (expressed as a mm/h equivalent) is the hydraulic conductivity. K-values determined with these tests are 21-112 mm/h. Slope angles (35°-45°) of the tested plots had no relation with the measured K-values. A relation was found between K and rainfall intensity i_r, as figure 20 shows. The relation was tested in the field by raining the same plot with three different rainfall intensities. For a rainfall intensity of 96 mm/h K was 25 mm/h; at 202 mm/h K was 49 mm/h and at 230 mm/h K was 57 mm/h. The increase of K with rainfall intensity may be caused by an extra hydraulic head, as more water is at the surface when more runoff occurs. However, splash loss may also be a factor: this probably is more or less linearly related to rainfall intensity. In natural rainfall, the net loss by splash will be zero. The K-values determined from these tests may be overestimated by perhaps another 10% because of loss of runoff at the runoff collection funnel. For rainfall intensities of ≤140 mm/h, a mean value of K = 46.8 mm/h was obtained, with a standard deviation s_K = 16.3 mm/h for 17 tests.

INFILTRATION ENVELOPES

Infiltration envelopes were obtained by connecting time-to-ponding points for different rainfall intensities. The spatial variability of the infiltration parameters K and S causes these points to lie 'spread' along a mean infiltration envelope rather than to be exactly on the envelope. Individual infiltration envelopes were constructed by fitting an exponential decay function:

$$i = K + e^{a-btp} \qquad (1)$$

where a and b are constants.

From this function K-values were obtained using linear regression after the function was transformed logarithmically:

$$\ln (i-K) = a - bt_p \qquad (2)$$

K-values obtained were 13.3-62.9 mm/h (table 6). The use of the logarithmic function however will always cause the calculated K-value to be less than the smallest i_r-value used, as (i - K) must be a positive value. Non-logarithmically transformed non-linear regression will be used in future K-calculations.

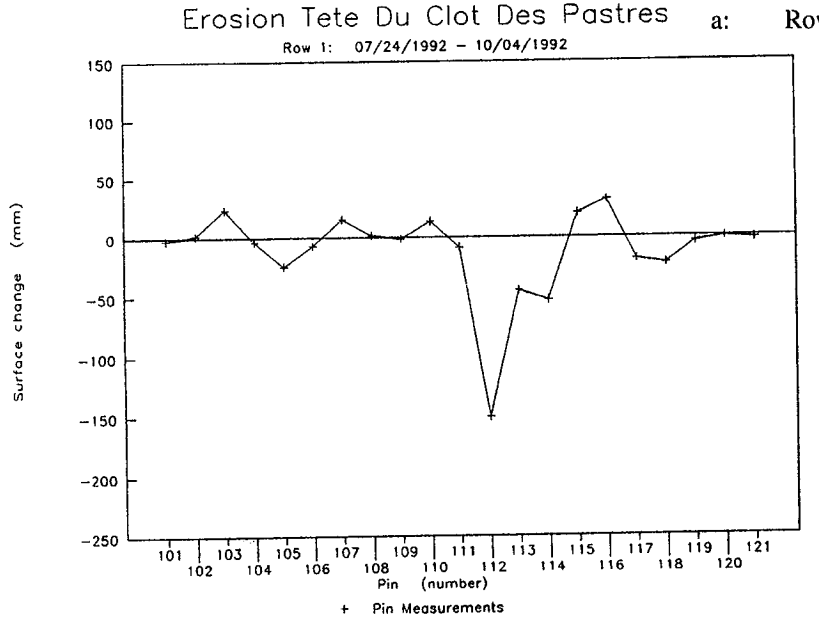

a: Row 1.

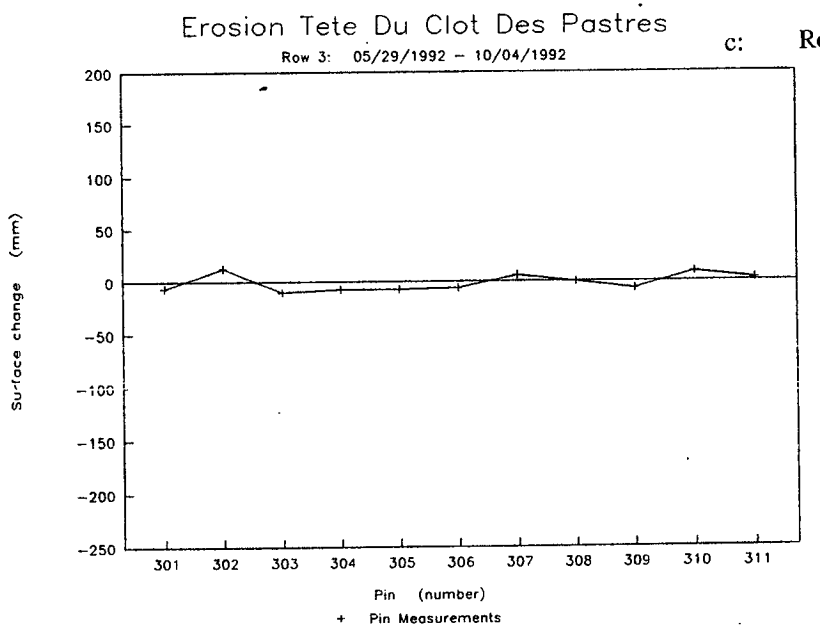

c: Row 3.

Figure 19: Surface level change in the monitored gully of the 'Tête du Clot des Pastres' debris flow source area between 29 may 1992 and 4 october 1992.
The location of the erosion marker rows is given in figure 11; erosion markers have rising numbers from northwest to southeast.

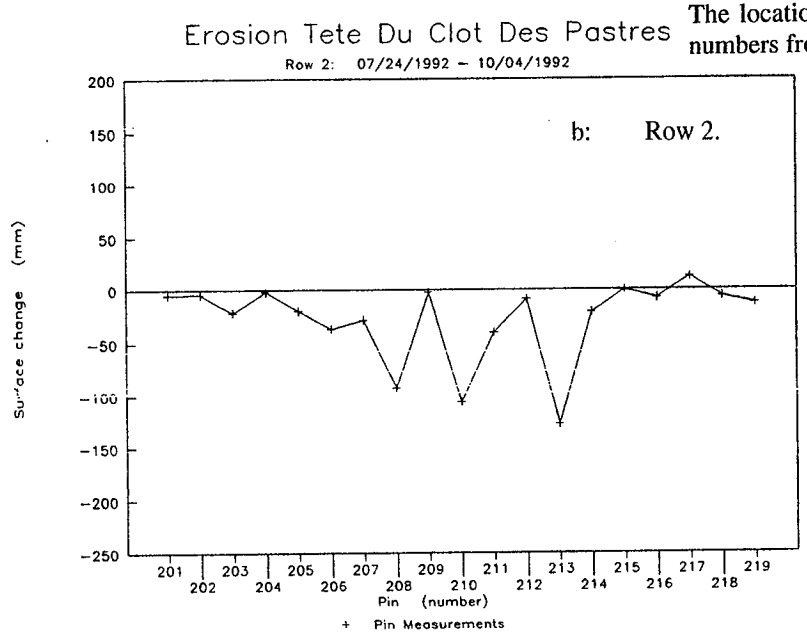

b: Row 2.

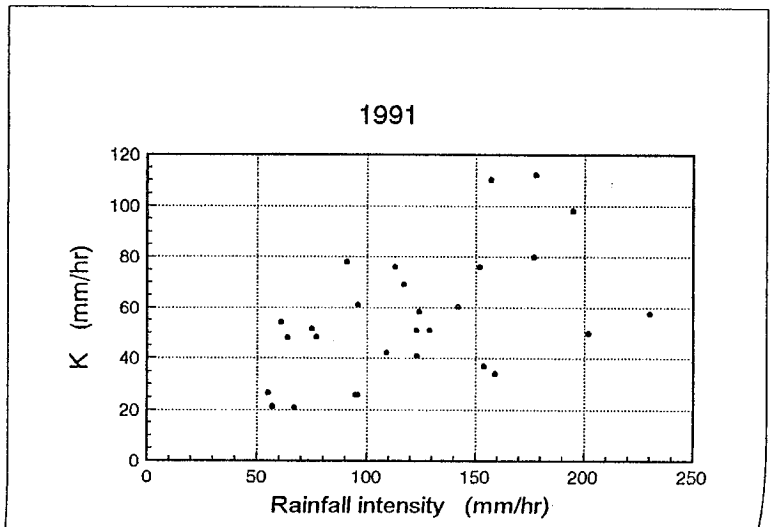

LOCATION	TEST NR	REGRESSION VALUES (equation 2) a	b	K	R^2
Tête du Clot des Pastres	1	5.05	0.0065	13.3	0.94
	2	5.87	0.0235	62.9	0.96
	3	6.14	0.0261	48.1	0.97
	4	5.93	0.0207	40.2	0.92
Pra Bouréou South	5	5.29	0.0112	56.5	0.97
	6	5.39	0.0100	38.8	0.98
	7	5.32	0.0122	37.1	0.97
Bayasse (Terres Noires)	8	5.35	0.0065	29.3	0.94

Table 6: Data obtained from exponential curve fitting to the infiltration envelope data.

The individual infiltration envelopes fitted to the data explain 92%-98% of the total variation in the data. Figure 21 shows the infiltration envelope data.

When all 1991 data points are put together, figure 22 a is obtained. A visual estimation of mean K from this diagram gives K≈42 mm/h (168 datapoints). These datapoints are not all for the same type of regolith: data from the Terres Noires marls, which have a more clayey regolith, are also represented in this diagram. Therefore, in figure 22 b distinction is made for the different source areas. The regolith parent material is the same for the Tête du Clot des Pastres and Pra Bouréou South debris flow source areas, and as can be seen these regoliths do not show any significant difference. The Terres Noires regolith may however be significantly different.

Figures 22 c and d give a differentiation of the 1991 data from the Tête du Clot des Pastres debris flow source area for surface type and soil wetness. Rills and interrills do not seem to have different times-to-ponding at comparable rainfall intensities. This may however be due to the relatively small surface (maximum about 20%) of a rill within a testplot which is still called a 'rill'-plot. Initial wetness of the regolith, qualitatively determined, also seems to have no effect on time-to-ponding.

The 1992 data from the Tête du Clot des Pastres area however seem to suggest a relation between time-to-ponding and soil wetness. The concentration of 1992-datapoints at low times-to-ponding for a fixed rainfall intensity (Fig.22 e) shows this relation, as most of these datapoints were obtained during the 'wet' period in june 1992. Such a relation may not be surprising, but was to be expected, as sorptivity depends on soil wetness. This follows from equation (27) in part I, where S depends on the pressure head h_f at the wetting front. The absence of a relation between surface type (rill - interrill) and time-to-ponding is confirmed by the 1992 data (Fig.22 f). This does not agree with Bryan (1978) who found smaller K-values in rills.

Rainfall simulations done in 1992 in the debris flow source area Combal du Menon do not differ significantly from the values determined at the Tête du Clot des Pastres site in 1992.

It is remarkable that the infiltration characteristics of the regolith in different debris flow source areas resemble each other so closely. Only the 1991 data from the Terres Noires marls seem to be significantly different. These data were not measured in a debris

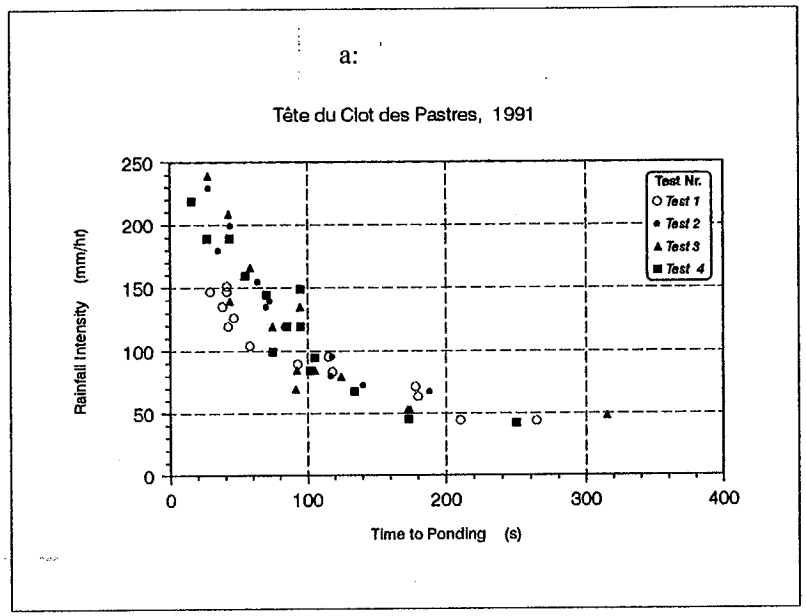

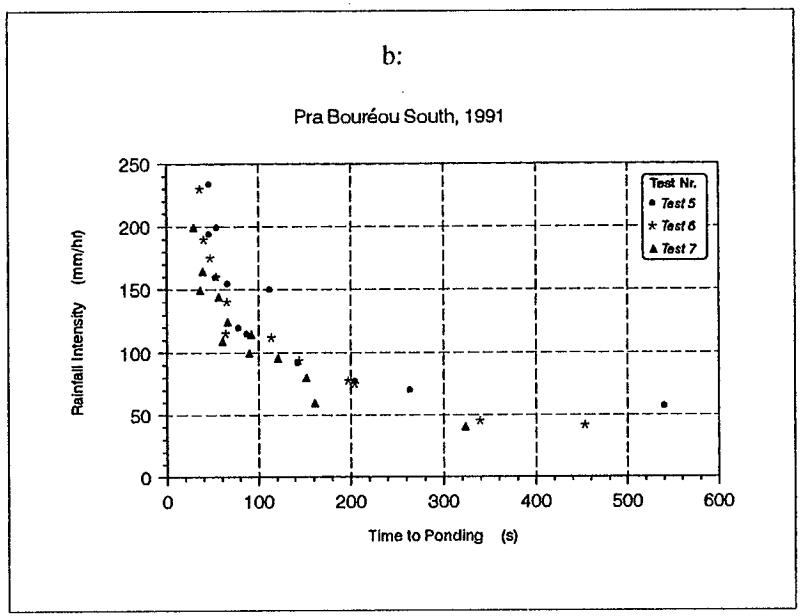

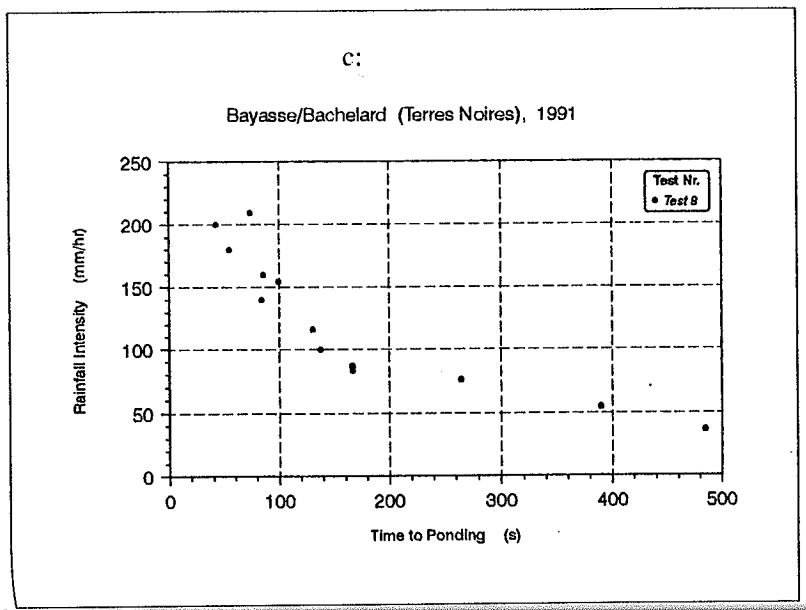

Figure 21: Infiltration envelopes from individual tests (1991).

a: 1991 data, no differentiation.

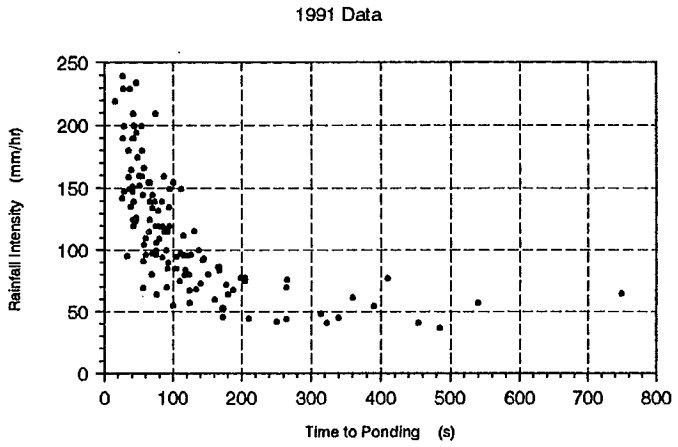

b: 1991 data, differentiated for source area (different parent material).

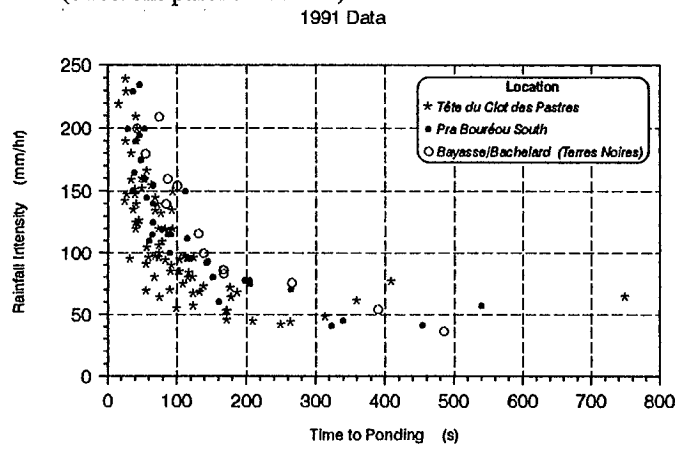

Figure 22: Influence of several factors on infiltration characteristics (time top ponding).

c: 1991 data, differentiated for surface type (rills vs. interrill areas).

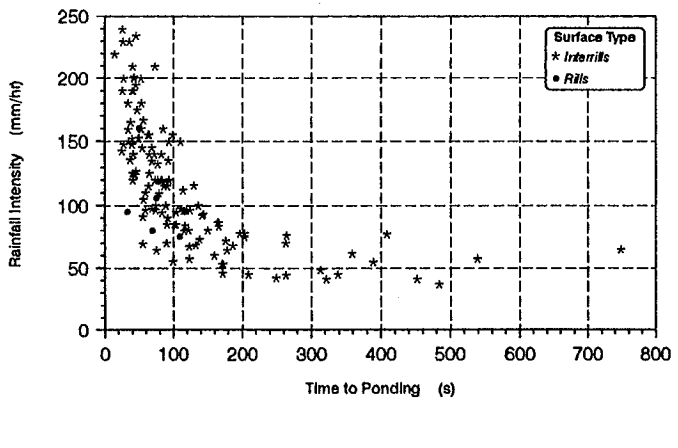

d: 1991 data, differentiated for initial soil wetness.

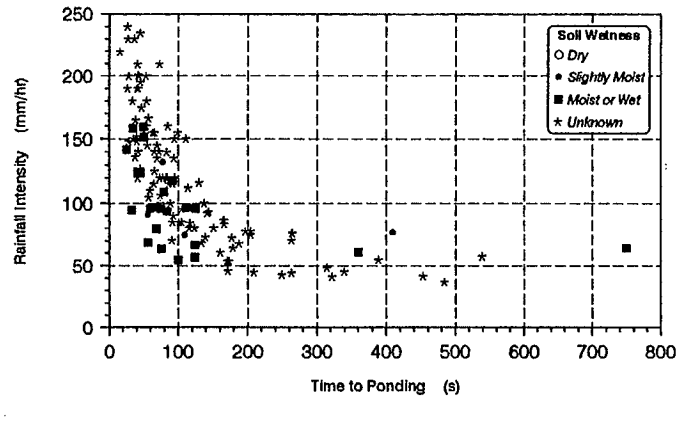

e: Tête du Clot des Pastres data, differentiated for year of testing (different initial soil wetness).

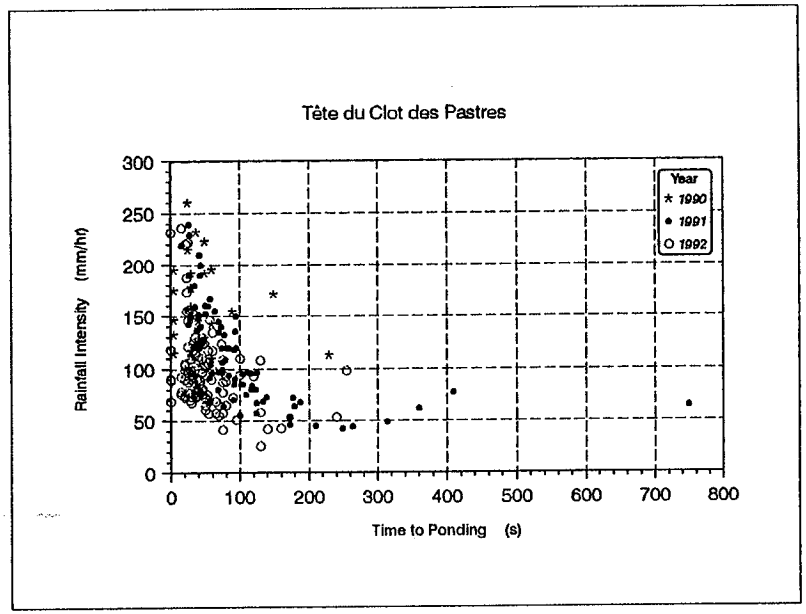

f: 1992 data, differentiated for surface type (rills vs. interrill areas).

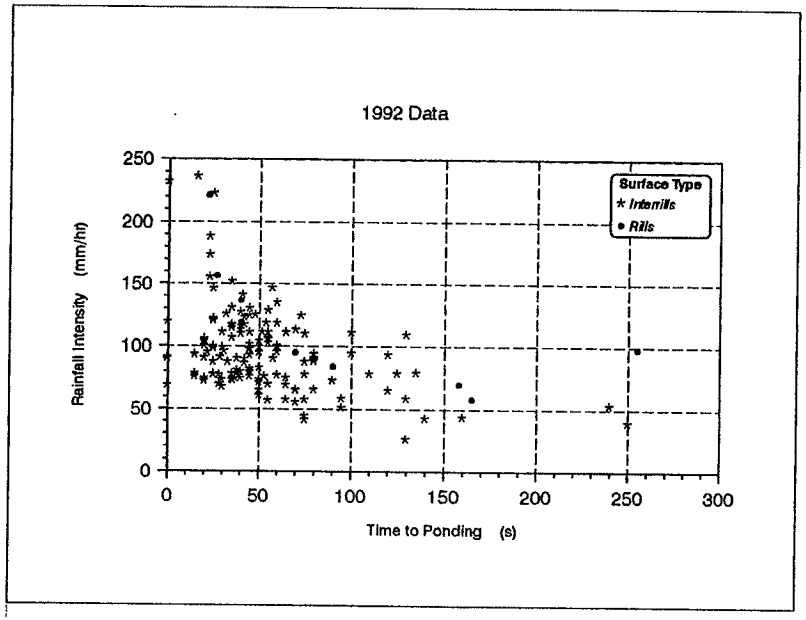

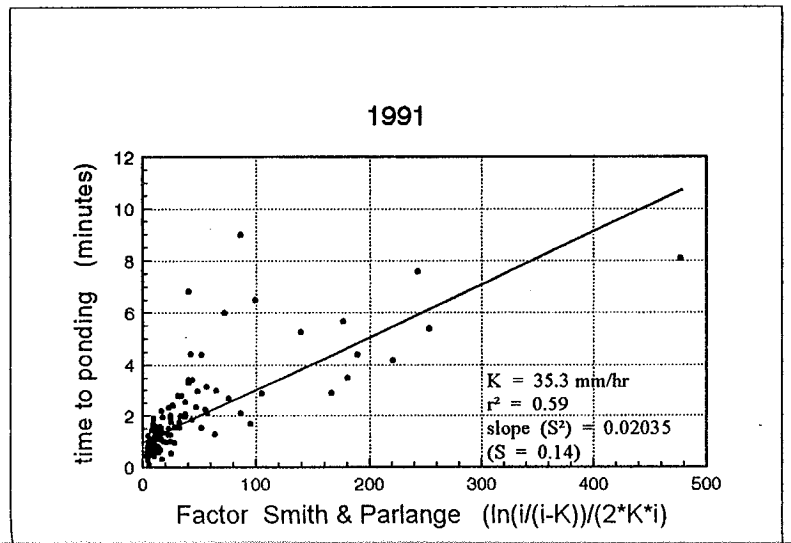

Figure 23: Sorptivity determined from regression using the Smith & Parlange equation (equation 28 in part I chapter 2)

flow source area. It might be, that comparable infiltration values are characteristic for debris flow source areas in the same climatic region.

COMPARISON OF CONSTANT RUNOFF AND INFILTRATION ENVELOPE METHODS

The values calculated for K by the constant runoff and the infiltration envelope methods are not equal. The mean K-value calculated from the infiltration envelope method is about 10% less than the value obtained from the constant runoff method. As has already been pointed out, this may for the larger part be caused by loss of runoff in the constant runoff tests. Besides, the depth of the water film present at the surface may cause an extra hydraulic head which increases the infiltration into the regolith. Table 7 gives some of the advantages and disadvantages of both methods.

TEST METHOD	ADVANTAGES	DISADVANTAGES
CONSTANT RUNOFF	1: K and S values are easy to calculate the field. 2: K and S are obtained from each test	1: Much water needed, as it takes a long time before constant overland flow discharge is obtained. This can problematic if water is sparse. 2: Not all overland flow is caught as some overland flow is lost by leakage of the flap 3: Number of actions involved during test (reading overland flow amount, time and water level; changing bottles; removing sediment; refilling simulator) makes it more snesitive for errors. Besides, more operators are needed (2-
INFILTRATION ENVELOPE	1: Only little water needed for tests 2: Less variable K and S values as these are mean values from multiple tests. 3: Mean K and S values over larger surface area determined	1: At least 10 tests are needed to obtain one infiltration envelope. For each test comparable sites must be used, which is not always possible. 2: Calculation of K and S is more difficult. These cannot be easily calculated in the field, making checks more difficult.

Table 7: Advantages and disadvantages of the Constant Runoff and the Infiltration Envelope methods.

SORPTIVITY VALUES

With K-values obtained from either the constant runoff or the infiltration envelope methods, sorptivity was calculated using the Smith & Parlange (1978) equation (28) (in part I). For K = 35.3 mm/h a mean sorptivity value S = 0.14 cm/√min (= 10.8 mm/√h) was obtained by linear regression (Fig.23). The regression is much influenced by the points that

Figure 23: Sorptivity determined from regression using the Smith & Parlange equation (equation 28 in part I chapter 2).

Factor Smith & Parlange (ln(i/(i-K))/(2*K*i)

lie far away from the origin. These points have rainfall intensities only slightly higher than the hydraulic conductivity. If these points are not taken into account for the regression, the obtained S-value would be higher. Sorptivity is not independent of the rainfall intensity: sorptivities increased from S = 0.1 cm/√min at lower rainfall intensities to 0.4 cm/√min at higher intensities.

MICROSCALE MASS MOVEMENTS

When rainfall simulation were done using high rainfall intensities (> 100 mm/h) on steep slopes (> 39°), a remarkable phenomenon was often observed: the saturated top layer of the regolith would fail and move downslope (Fig.24). When it occurred, it always occurred in the first minutes of the tests, when the surface was already saturated and runoff was present, but the microrelief was not yet smoothed by splash and runoff processes. Usually these masses moved as a flow.

An even more spectacular phenomenon was observed if the simulation was done on a rill. In such cases the micro-scale mass movements moved into the rill, got concentrated there and might then transform into a miniature debris flow, if enough water was taken up into the mass. Such miniature debris flows could move up to several metres outside the tested plot. Figure 25 shows such a miniature debris flow.

The initiation of the micro-scale mass movements seems to follow the initiation mechanism described by Takahashi (1978, 1980, 1981): the mass spontaneously starts moving as a flow when it is saturated and a water film is present at the surface. The transformation into a miniature debris flow is caused by the concentration of these debris masses in a rill and uptake of additional water into the masses during movement. The miniature debris flows, which contain only the fine-grained material present in the regolith, seem to have a laminar flow regime.

The conditions for the occurrence of these small mass movements appear to be:

slope angles >39°.
rainfall intensity >100 mm/h on interrill areas, and >80 mm/h on rills. The lesser rainfall intensities needed for rills may possibly be caused by the concentration of water in rills.
quick softening of the surface crust when rainfall starts.
the presence of a pronounced microrelief at the surface.

When a combination of slope angle and rainfall intensity was used, the best discrimination was found between mass movement occurrence and no mass movements. Figure 26 shows the diagram of the occurrence of these mass movements. Most side slopes of the monitored gully in the Tête du Clot des Pastres debris flow source area have slope angles of 40°. This means that microslumps may occur on these slopes at rainfall intensities of around 100 mm/h or more.

Figure 24: Microscale debris slide initiated during a rainfall simulation.

Figure 25: Microscale debris flow initiated during a rainfall simulation.

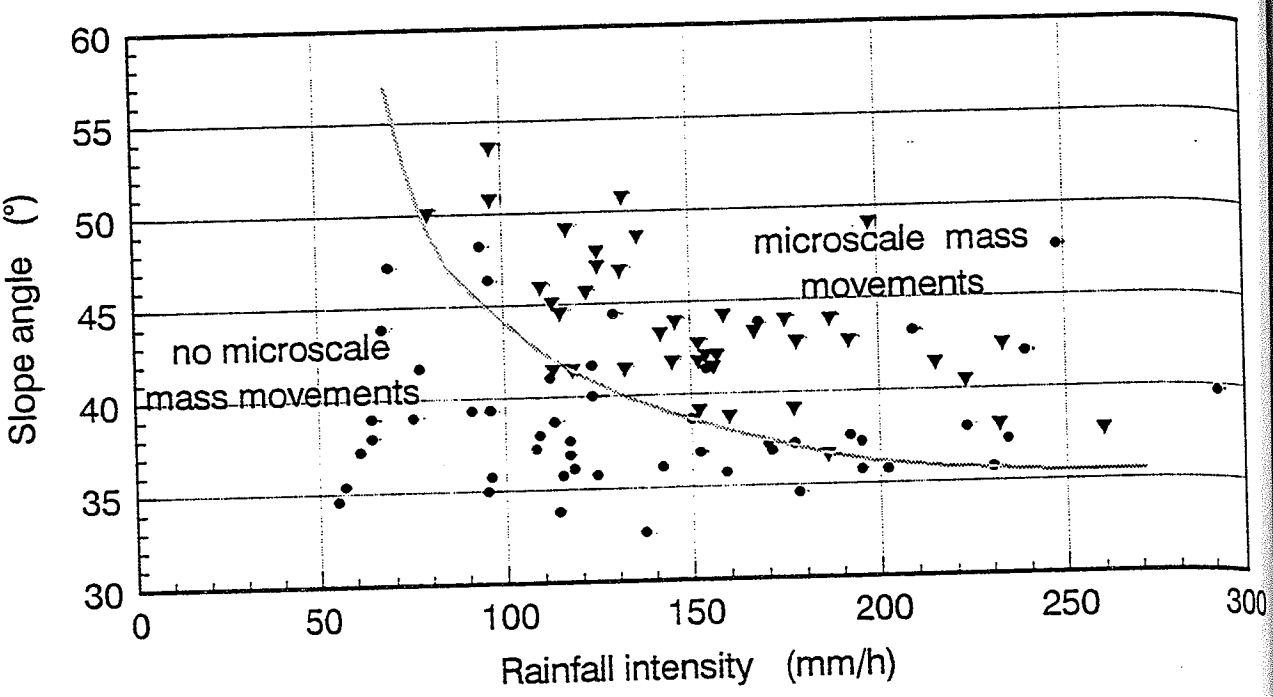

Figure 26: The occurrence of microscale mass movements (slides and flows) in relation to surface slope angle ßand rainfall intensity i_r.

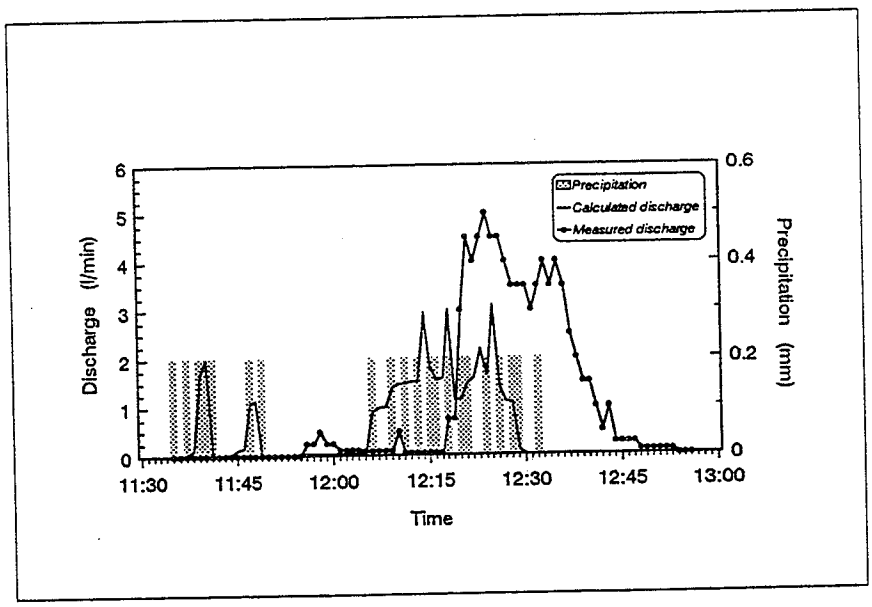

Figure 27: Calculated and measured overland flow intensities at the hydrologic monitoring site in the 'Tête du Clot des Pastres' debris flow source area.

RUNOFF MONITORING

The hydrologic monitoring unit (part I, Fig.2) records the surface runoff of a subcatchment within the Tête du Clot des Pastres debris flow source area (Figs.8, 10 and 11). This subcatchment is 30 m long, maximally 10 m wide and covers an area of 200 m². The mean slope of the gully is 40°, slope angles of the side slopes vary from 35°-53°.

The recorded discharge values were not always reliable. At higher discharges the sediment transported by/with the flowing water would obstruct the flume. This phenomenon could be seen in the data: when the flume got obstructed, recorded discharge would suddenly drop to (near) zero, instead of the normal gradual decrease of discharge. Later removal of the debris, either by failure of a debris mass or by streamflow erosion, would be shown by the sudden (re)start of discharge. This pattern in runoff recordings has been found several times. If too much debris had accumulated in and behind the flume, filling this completely, any more supply of water and debris would flow over the edges of the flume, not recorded by the discharge gauges. Video camera recordings of runoff events in 1992 (august 19th and 29th) support this interpretation of the data.

Still, for some events reliable runoff data have been obtained, mostly for lesser runoff events. A clear difference has been found in the response of the catchment for 'wet' and 'dry' periods. In the wet period the regolith would remain very wet even when no rain had fallen during two or three days, whereas in the dry period the regolith would have recovered from a rainfall event after one or two days. The rainfall intensities causing overland flow are also quite different for the 'wet' and the 'dry' periods. Table 8 presents some of the data. In wet periods, rainfall intensities «10 mm/h have produced overland flow. It seems probable that saturation overland flow may have contributed to the runoff in these circumstances. In dry periods, the minimum rainfall intensity needed for overland flow seems to be in the order of 15 mm/h during 10 minutes. These intensities are well below those determined from rainfall simulations. It may well be that the infiltration capacity of the gully floor is much less than that of the regolith on the gully side slopes. Regolith depth is less in gullies than on the side slopes: sometimes bedrock outcrops in the gully, and this probably has a much smaller infiltration capacity than the regolith.

'WET' PERIOD	'DRY' PERIOD
2 mm/hr during 15 minutes	6 mm/hr during 10 minutes
2.5 mm/hr during 50 minutes	15 mm/hr during 10 minutes
3 mm/hr during 10 minutes	20 mm/hr during 5 minutes
6-8 mm/hr during 25 minutes	24 mm/hr during 6 minutes
8 mm/hr during 30 minutes	24 mm/hr during 10 minutes
12 mm/hr during 15 minutes	30 mm/hr during 10 minutes
	35 mm/hr during 5 minutes
	40 mm/hr during 5 minutes

Table 8: Some examples of rainfall intensities producing overland flow: differences between 'wet' and 'dry' periods.

HYDROLOGIC MODELLING

The modelling of the hydrologic respons of the instrumented catchment using a DTM and the PC-RASTER GIS-software has not yet been satisfactory. Figure 27 shows the result of one model run. The model shows several shortcomings:

Total event runoff was usually underestimated.

The model runoff reacts much quicker on rainfall variations than the measured runoff. This problem is probably caused by the PC-RASTER module WATERSHED, which transports the total amount of surface water one pixel downstream every time-step.

If subsurface flow is also taken into account, the model results in a continuous increase of runoff for a long time. This is not so strange, taken the fact that the underlying bedrock is impervious (K = 0) in the model, so all the rainfall has to flow out at the outlet point.

The discharge is overestimated at the start of high-intensity rainfall, and underestimated during peak discharges. The last is caused by the non-discrimination between (laminar) sheetflow and the much faster (turbulent) rillflow. The longer residence time of the water on the slopes in the model will cause more loss by infiltration.

THE RESULTS OF DEBRIS FLOW FREQUENCY MODELLING

In part II a run out model was proposed which was based on the assumption that run out distance of the debris flow mass is determined by:

- The initial slope angle in relation to the static friction angle of the debris mass which determines the amount of water and thus the excessive pore pressure in the flowing mass.

- The mobile friction angle in relation to the excessive pore pressure which determines the slope angle where the debris mass will stop.

It is further assumed that there is no loss of ground water at least in the centre of the debris flow and that there is enough mass available to reach the critical slope angle at the end of the flow path.

Detailed morphological observations were made on seven debris flows in the basin of Barcelonnette (Van Steijn et al., 1988) and the results are used for testing the run out model. Figure 28 shows a plot of the slope angle of initiation of these debris flows against the slope angle where the debris flows have stopped according to the observations made by Van Steijn et al (1986). The points in the graph are fitted with the theoretical θ_{in} - θ_{res} line which can be obtained from equation (46). The initial static friction angle of the debris was determined in the field while the mobile friction angle was back analyzed using equation 45 and assuming that the excessive pore pressure ratio was 0.8 (see Sassa, 1988).

The figure shows apart from two outliers in the right upper part of the graph a good correlation between observed and calculated relationships. The outliers proved to be two debris flows which were obstructed by a deep gully crossing the flow path.

CONCLUSIONS AND RECOMMENDATIONS

The investigations into the mechanisms of debris flow initiation have so far led to the following conclusions:
Debris flows in the study area are mainly caused by short-duration high-intensity rainstorms.

These rainstorms are usually a local phenomenon. The spatial and temporal occurrence of debris flows may therefore possibly reflect the occurrence of these rainstorms.

Spatially more extensive rainstorms which have moderate to high intensities and long duration, as the exceptional situation that occurred end september 1992, can initiate several debris flows within a larger area.

Overland flow only occurs if rainfall intensity is high enough and lasts long enough. The mean threshold intensity for the occurrence of overland flow as determined from rainfall simulations is about 42-47 mm/hr during at least 5 minutes. A wide scatter of values around the mean has been found. Runoff recorded by the automatic hydrologic monitoring unit however suggests a much lower threshold value: about 15 mm/hr during at least 10 minutes. Infiltration excess overland flow seems the most probable mechanism producing overland flow in this situation, because the regolith storage capacity is usually more than 100 mm between field capacity and saturation (440 mm regolith depth times 0.30 water content difference between field capacity and saturation).

If the regolith is very wet after a prolonged period of rainfall, the threshold rainfall intensity for the occurrence of debris flows is much lower: the value can be as low as 3 mm/h as appeared from the runoff recordings. Threshold values of rainfall intensity determined from rainfall simulations are higher, but slightly less than the values determined for dry regolith in rainfall simulations. Saturation overland flow may be the responsable mechanism for overland flow production in this situation.

The infiltration capacity during the first minutes of rainfall of dry regolith is much higher than the threshold values mentioned. This means that the threshold value for the occurrence of overland flow is much higher during the first minutes. It is caused by the sorptivity of the regolith. Mean sorptivity values measured were 0.14cm/ $\sqrt{}$min.

In dry regolith the crusted surface, cemented by lime, quickly softens when rainfall starts.

The infiltration characteristics K and S appear to be quite similar for regoliths in all surveyed debris flow source areas. Only the infiltration characteristics of a slope in Terres Noires marls regolith seems to be significantly different. This slope was not part of a debris flow source area. The similarity of debris flow source area regolith infiltration

characteristics may possibly be a characteristic property for debris flow source areas.

With increasing overland flow discharge, an increasing amount of material is transported. A threshold value of overland flow discharge, still unknown quantitatively, must be exceeded to initiate a debris flow.

Very high rainfall intensities (> 100 mm/h) on very steep slopes (> 39°) during several minutes may initiate micro-scale mass movements of maximally several hundreds of cm^3 of volume. The mass movements are flow-like and seem to be initiated according to the mechanism described by Takahashi (1978, 1980, 1981). Continuing their way downslope they may dilate by incorporation of additional water and become miniature debris flows or transform into sediment-rich overland flow. This is observed more often in rills than on inter-rill areas.

The mean total surface lowering in the regolith may be > 3 cm/y. The major part of it may be removed during summer by infiltration excess overland flow.

In summer rills and gully floors become more pronounced and get sharper contours. This is caused by overland flow.
In spring, during the snowmelt season, the high amount of water from snowmelt and rain can saturate the regolith and cause solifluction. The solifluction masses move towards the gully, where they accumulate. These masses are usually removed in summer.

When such sediment-rich runoff or micro-scale debris flows reach the coarse debris accumulations in the main drainage channel, it can either enter that debris and flow through the pores, or it can run over it.

Whether or not overland flow, containing a lot of sediment, can flow through the pores of the coarse debris, depends on the pore size distribution of the coarse debris and the grain size distribution of the 'fine-grained' sediment in the overland flow/debris flow.

The coarse debris may be destabilized by the build-up of pore pressure if runoff flows through the pores. In this case the initiation model of Postma (1988) seems valid. Impact and loading forces may also initiate the movement, if the sediment-rich runoff runs over the coarse debris. Therefore the model of Postma (1988) will be adjusted, according to the flow chart given in figure 29.

The cohesionless coarse debris has a dynamic angle of internal friction ϕ_d of 36°-39°. The variation in ϕ_d seems to be caused mainly by material sorting, parent material is less important.

Debris flows from the Tête du Clot des Pastres debris flow source area seem to be initiated by rainfall with peak intensities over 50 mm/h.

Frequency of debris flows can only be obtained from a model if the initiation conditions for debris flow can be calculated and if enough detailed rainfall data are available. A rainfall intensity-frequency-duration curve is needed, which cannot be derived from daily rainfall totals.

Figure 28: Calculated and observed threshold (theta-rest) angles for run out of 7 debris flows in the French Alps.

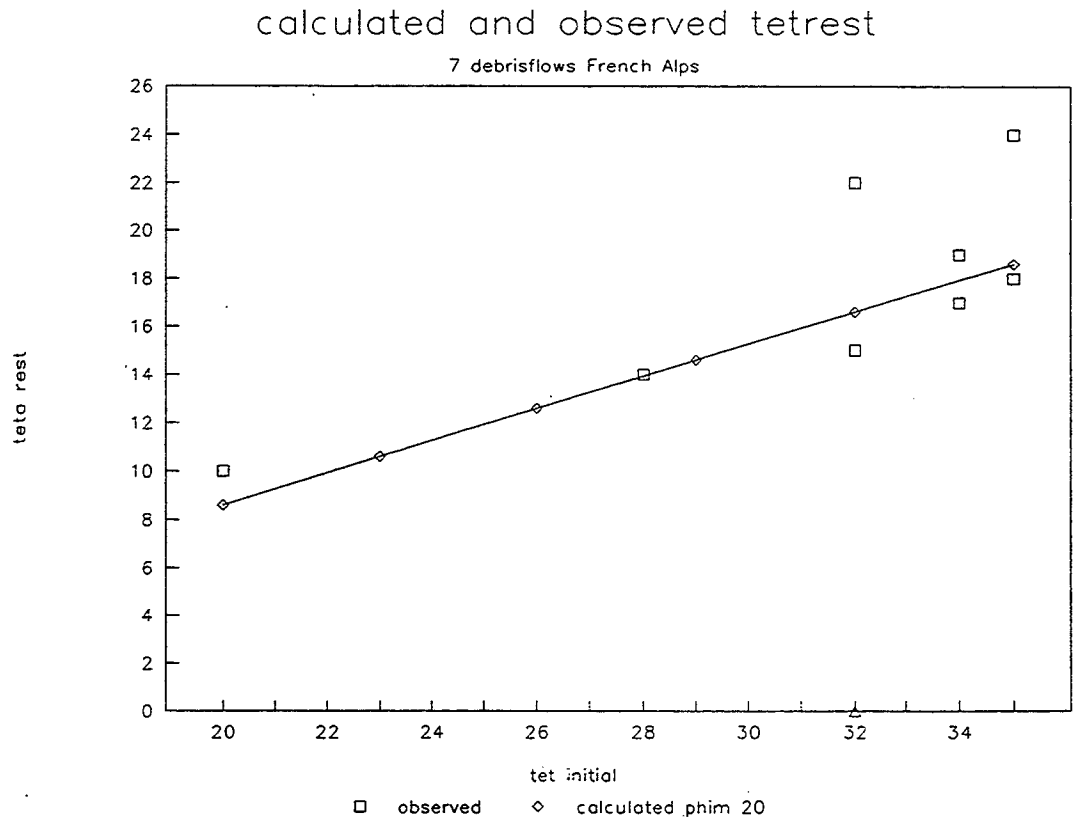

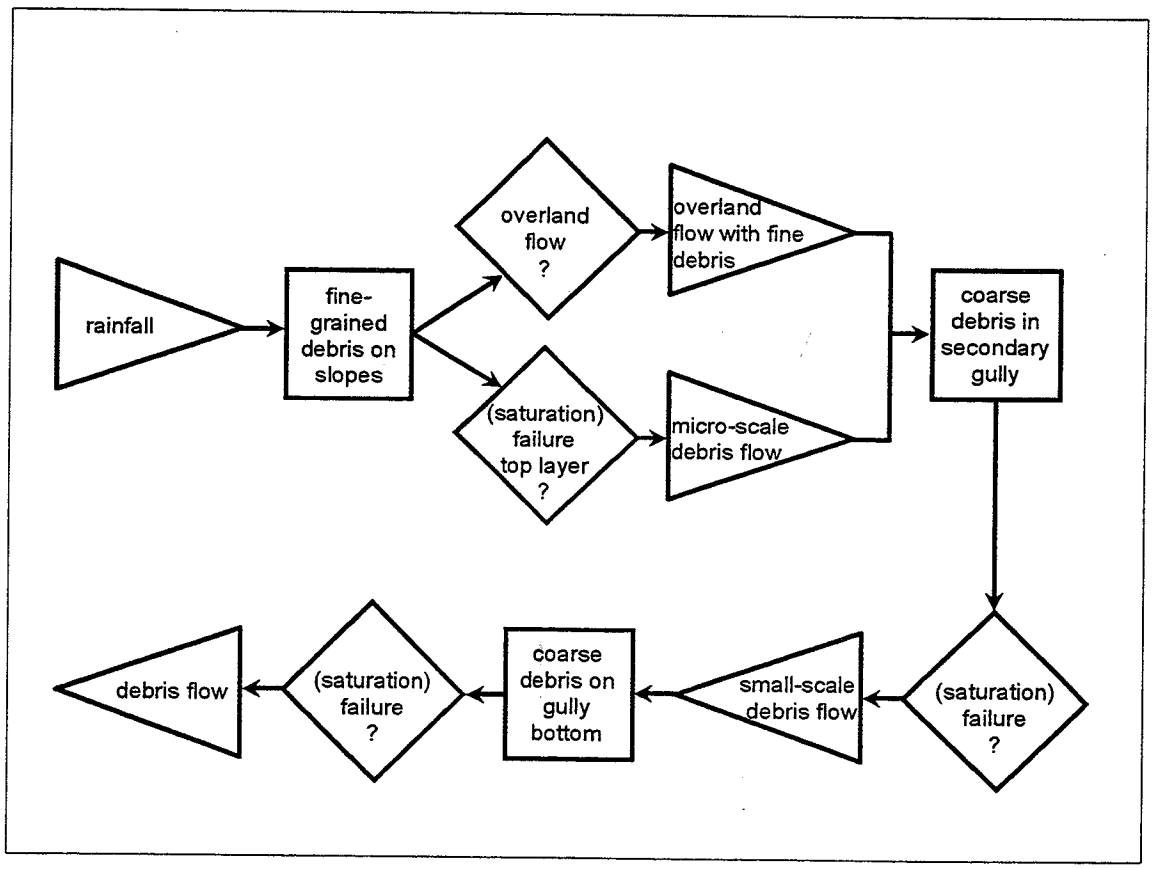

Figure 29: Adjusted flow chart of debris flow intitiation.

REFERENCES

BRYAN R.B., YAIR A.& HODGES W.K. 1978. *Factors controlling the initiation of runoff and piping in Dinosaur Provincial Park badlands, Alberta, Canada.* Zeitschrift für Geomorphologie, Neue Folge, Supplementband 29, pp. 151-168.

COSTA J.E. 1984. *Physical geomorphology of debris flows.* In: Costa, J.E. & P.J. Fleisher (eds.): Developments and Applications of Geomorphology, Springer Verlag, Berlin/Heidelberg, 372 pp. (pp.268-317).

DOUGUEDROIT A. & DE SAINTIGNON M.-F. 1970. *Méthode d'étude de la décroissance des températures en montagne de latitude moyenne: exemple des Alpes françaises du Sud.* Revue de Géographie Alpine, nr. 58, pp. 453-472.

HOVIUS N. 1990. *Ontstaan van puinstromen. Een onderzoek naar de aard van ontstaansgebieden van puinstromen en naar de manier waarop puinstromen ontstaan, in het zuidelijk deel van de Franse Alpen.* Unpublished report Utrecht University, Department of Physical Geography, 122+69 pp. (in dutch).

INNES J.L. 1983. *Debris flows.* Progress in Physical Geography, vol. 7, nr. 4, pp. 469-501.

PIERSON T.C. 1980. *Erosion and deposition by debris flows at Mt. Thomas, North Canterbury, New Zealand.* Earth Surface Processes, vol. 5, pp. 227-247.

PIERSON T.C. 1981. *Dominant particle support mechanisms in debris flows at Mt. Thomas, New Zealand, and implications for flow mobility.* Sedimentology, vol. 28, pp. 49-60.

POSTMA R. 1988. *Model voor de initiatie van debris flows.* Unpublished report Utrecht University, Department of Physical Geography, 20 pp. (in dutch).

SASSA K. 1988. *Geotechnical model for the motion of landslides.* In C.Bonnard, Landslides. Proceedings of The Vth International Symposium on landslides, Lausanne.Balkema, Rotterdam, pp37-56.

SMITH R.E. & PARLANGE. J.Y. 1978. *A parameter-efficient hydrologic infiltration model.* Water Resources Research: a Journal of the Sciences of Water, vol. 14, nr , pp. 533-538.

TAKAHASHI T. 1978. *Mechanical characteristics of debris flow.* Journal of the Hydraulic Division, Proceedings ASCE, vol. 104, nr. HY8, proc. paper 13971, pp. 1153-1169.

TAKAHASHI T. 1980. *Debris flow on prismatic open channel.* Journal of the Hydraulic Division, Proceedings ASCE, vol. 106, nr. HY3, proc. paper 15245, pp. 381-396.

TAKAHASHI T. 1981. *Debris flow.* Annual Review of Fluid Mechanics, vol. 13, pp. 57-77.

VAN STEIJN H. 1988. *Debris flows involved in the development of Pleistocene stratified slope deposits.* Zeitschrift für Geomorphologie, Neue Folge, Supplementband 71, pp. 45-58.

VAN STEIJN H., DE RUIG J. & HOOZEMANS F. 1988. *Morphological and mechanical aspects of debris flows in parts of the French Alps.* Zeitschrift für Geomorphologie, Neue Folge, Band 32, nr. 2, pp. 143-161.

VAN STEIJN H. 1991. *Frequency of hillslope debris flows in a part of the French Alps.* Bulletin of Geomorphology, nr. 19, pp. 83-90.